THE JOURNAL OF IMMUNOLOGY

Changing the Antigen Binding Specificity by Single Point Mutations of an Anti-p24 (HIV-1) Antibody

Karsten Winkler, Achim Kramer, Gabriele Küttner, Martina Seifert, Christa Scholz, Helga Wessner, Jens Schneider-Mergener and Wolfgang Höhne

J Immunol 2000;165;4505-4514

The Journal of Immunology is published twice each month by
The American Association of Immunologists, Inc.,
9650 Rockville Pike, Bethesda, MD 20814-3994.

Print ISSN: 0022-1767 Online ISSN: 1550-6606.

Changing the Antigen Binding Specificity by Single Point Mutations of an Anti-p24 (HIV-1) Antibody[1]

Karsten Winkler,* Achim Kramer,† Gabriele Küttner,* Martina Seifert,† Christa Scholz,* Helga Wessner,* Jens Schneider-Mergener,† and Wolfgang Höhne[2]*

The murine mAb CB4-1 raised against p24 (HIV-1) recognizes a linear epitope of the HIV-1 capsid protein. Additionally, CB4-1 exhibits cross-reactive binding to epitope-homologous peptides and polyspecific reactions to epitope nonhomologous peptides. Crystal structures demonstrate that the epitope peptide (e-pep) and the nonhomologous peptides adopt different conformations within the binding region of CB4-1. Site-directed mutagenesis of the fragment variable (Fv) region was performed using a single-chain (sc)Fv construct of CB4-1 to analyze binding contributions of single amino acid side chains toward the e-pep and toward one epitope nonhomologous peptide. The mutations of Ab amino acid side chains, which are in direct contact with the Ag, show opposite influences on the binding of the two peptides. Whereas the affinity of the e-pep to the CB4-1 scFv mutant heavy chain variable region $Tyr^{32}Ala$ is decreased 250-fold, the binding of the nonhomologous peptide remains unchanged. In contrast, the mutation light chain variable region $Phe^{94}Ala$ reduces the affinity of the nonhomologous peptide 10-fold more than it does for the e-pep. Thus, substantial changes in the specificity can be observed by single amino acid exchanges. Further characterization of the scFv mutants by substitutional analysis of the peptides demonstrates that the effect of a mutation is not restricted to contact residues. This method also reveals an inverse compensatory amino acid exchange for the nonhomologous peptide which increases the affinity to the scFv mutant light chain variable region $Phe^{94}Ala$ up to the level of the e-pep affinity to the wild-type scFv. *The Journal of Immunology,* **2000, 165: 4505–4514.**

Antibodies are developed during evolution as a sophisticated system for specific Ag recognition and are generally thought to make highly specific Ab-Ag interactions. In contrast, polyreactivity is a known feature of natural autoantibodies (NAA)[3] found in sera of healthy humans and rodents as well as in lower phylogenetic species (1, 2). Affinity maturation of Abs can be considered a fast mini-evolution of a specific binding behavior and is well understood from the immunological point of view (3). Nevertheless, the structural features underlying the differences between specificity and polyreactivity are poorly understood at the molecular level (4, 5).

Ag binding of Igs is mediated by atomic interactions within complementary surfaces between Ab (paratope) and Ag (epitope). This high complementarity of the Ag combining site of an Ab is accomplished by residues from six hypervariable loops of complementarity-determining regions (CDRs), contributed by the heavy (V_H) and light chain (V_L) variable domains (6). Comparative structural analysis of the main-chain conformation of the CDRs showed that five of them (L1, L2, L3, H1, and H2) preferentially adopt distinct backbone conformations, also termed "canonical structures" depending on the length of each loop and the nature of a few key residues (7, 8). In the Ag binding region the major determinants of specificity and affinity for an Ag are as follows: 1) the canonical structures of the CDRs; 2) the size, shape, and chemical features of their surface exposed residues; 3) their position relative to each other; and 4) the length and conformation of the H3-loop (9–11).

Inspecting crystal structures of Ab-Ag complexes reveals usually 15–20 directed interactions between the individual residues in the contact interface, which bury a surface between 160 and 900 $Å^2$ (11). Nevertheless, the contribution of single amino acid positions to overall affinity usually becomes inapparent in crystal structures. Only the substitution of residues within the paratope and epitope together with detailed binding studies allows the identification of the binding contribution of individual amino acid positions. Several mutational analyses of Ab binding regions were performed during the last years (12–18). They elucidate that Abs can use different strategies to accomplish high affinity and specificity, enthalpy mediated on the one hand or entropy mediated on the other hand (18–21). Furthermore, it became evident that four to six amino acids make the largest contribution to the free energy of binding (6, 18).

Despite the high affinity and selectivity typical for the interaction of Abs with their Ag, the phenomena of cross-reactivity (recognition of homologous structures) and polyspecificity (binding of epitope-unrelated structures) are observed quite frequently (5, 13, 22–27).

We used the well-characterized murine mAb CB4-1 for investigations on the structure-function relationship of Ab-Ag interaction. The subtype of this mAb was immunochemically identified as IgG2a/κ. The mAb CB4-1 recognizes the peptide epitope GAT PQDLNTML corresponding to the aa 46–56 of the HIV-1 capsid protein p24 (28, 29) and was used to analyze multiple binding capabilities of an affinity-maturated mAb by means of synthetic combinatorial peptide libraries (24) and crystal structure analysis

*Institute of Biochemistry and †Institute of Medical Immunology, Medical Department, Humboldt University, Berlin, Germany

Received for publication December 6, 1999. Accepted for publication July 28, 2000.

The costs of publication of this article were defrayed in part by the payment of page charges This article must therefore be hereby marked *advertisement* in accordance with 18 U.S.C. Section 1734 solely to indicate this fact.

[1] This work was partly supported by Deutsche Forschungsgemeinschaft Grants Ho1377/1, Ho1377/2, and SCHN317/6-1.

[2] Address correspondence and reprint requests to Dr. Wolfgang Höhne, Institut für Biochemie des Universitätsklinikums Charité der Humboldt-Universität zu Berlin, Monbijoustrasse 2, D-10117 Berlin, Germany E-mail address: wolfgang.hoehne@charite de

[3] Abbreviations used in this paper: NAA, natural autoantibodies, CB4-1, murine monoclonal anti-p24 (HIV-1) Ab; CDR, complementarity-determining region; e-pep, epitope peptide; u-pep, epitope unrelated peptide; V_L, light chain variable region; V_H, heavy chain variable region; wt, wild type; Fv, fragment variable, sc, single-chain; IPTG, isopropyl-β-D-thiogalactopyranoside.

0022-1767/00/$02.00

(30). From cellulose-bound positional-scanning combinatorial libraries, five peptides were selected that are able to compete with the natural epitope peptide (e-pep) for binding to CB4-1 (24, 31). One of these library-derived peptides has a sequence related (homologous) to the epitope; whereas the sequences of the other peptides are completely unrelated (nonhomologous). It was demonstrated that even an Ab with high affinity toward its epitope is able to bind completely different peptides by interaction with unequal sets of "key residues" with comparable affinities (22–24). The term key residues defines those positions in the peptide which cannot be substituted (or can only be exchanged by physicochemically related amino acids) without substantial loss of peptide binding. It was suggested to discriminate between the term cross-reactivity, which means that the binding of homologous molecules is based on the same key residues, and the term polyspecificity, which is characterized by specific interaction with nonhomologous molecules mediated by different sets of key residues (24). The CB4-1 Fab was crystallized without and in complex with four different peptides, and x-ray structural analysis was performed to a final resolution of 2.6 Å (30). The crystal structures demonstrate that unrelated peptides adopt different conformations within the Ab-Ag complex and also form their critical contacts with different Ab side chains. Only small movements are observed in the framework of the Fab upon binding.

Here we investigate the binding contribution of two contact residues and one noncontact residue of the CB4-1 binding region and their individual influences on the specificity of peptide recognition for an epitope-related and an unrelated (nonhomologous) peptide. The variable region of CB4-1 was cloned into a vector which permits periplasmic expression of the CB4-1 scFv in *Escherichia coli*. Three single amino acid exchanges were introduced in this scFv by site-directed mutagenesis. The binding behavior of the expressed and purified scFvs was compared with the unmutated scFv using competition ELISA and substitutional analysis for the two structurally unrelated peptides. The latter method also allowed the detection of an inverse compensatory amino acid substitution in the epitope nonhomologous peptide, which was additionally characterized by competition ELISA. The structural and immunological impact of the results is discussed.

Materials and Methods

Reagents

All chemicals were of analytical grade. Restriction enzymes were purchased from Roche Diagnostics (Mannheim, Germany). Oligonucleotides were obtained from TIB-MOLBIOL (Berlin, Germany). Peptides were synthesized according to standard Fmoc protocols using a multiple peptide synthesizer (Abimed Analyse-Technik, Langenfeld, Germany) and analyzed by reverse-phase HPLC and matrix-assisted laser desorption ionization-time of flight mass spectrometry. In the e-pep, norleucine (= n) was introduced instead of methionine to prevent oxidation during peptide storage and handling in solution. It was shown earlier that this exchange has no influence on the peptide affinity to CB4-1 (29).

Amplification, cloning, and sequencing the variable region of CB4-1

The fusion of cells and the hybridoma selection were conducted as described earlier (28). The preparation of mRNA from the hybridoma cell line CB4-1/1F7 and the reverse transcription of cDNA was performed as described (32).

According to Jones and Bendig (33), PCRs were set up using the mouse heavy chain variable region leader sequence primers and the Cγ constant region primer (Cγ15 = 5′-GGCCAGTGGATAGAC; Pharmacia-LKB, Uppsala, Sweden) for the heavy chain amplification. PCRs were performed with mouse κ light chain variable region primers and the Cκ constant region primer (Cκ17 = 5′-TGGATGGTGGGAAGATG; Pharmacia-LKB) for the light chain amplification. Amplifications were conducted as described (32). The PCR fragments were purified on a 1% agarose gel, extracted by Qiaex (Qiagen, Chatsworth, CA) and cloned into the PCR II vector according to the TA cloning system protocol (Invitrogen, San Diego, CA). The nucleotide sequences are stored at the European Molecular Biology Laboratory Nucleotide Sequence data base under the accession numbers Z50145 for the CB4-1 V_H region and Z50146 for the CB4-1 V_L region.

Cloning and expression of the CB4-1 scFv in E. coli

For the expression of the CB4-1 Fv in *E. coli*, the variable regions were assembled by an oligonucleotide coding for a flexible linker fragment to form a scFv (V_H-$(Gly_4Ser)_3$Ala-V_L) by PCR as described (34). After a second PCR, which introduced a *Sfi*I site at the 5′ end and a *Not*I site at the 3′ end, the scFv construct was ligated into the *Sfi*I-*Not*I-cleaved phagemid pHEN1, including the myc tag for detection and purification purposes (35). The resulting vector pHEN 4-1 was used for the expression of soluble scFv into the periplasm of *E. coli* using the PelB signal peptide. For detection and purification the Ab 9E10 (Boehringer Mannheim, Mannheim, Germany) recognizing the myc tag was applied.

Examination of expression conditions has shown in our case that expression levels mainly depend on low isopropyl-β-D-thiogalactopyranoside (IPTG) concentrations and the choice of the *E. coli* strain. The most suitable *E. coli* strains were W3110, TG1, JM109, and XL1 (in the order of the expression level).

Production of scFvs was performed using the pHEN 4-1 vector in the *E. coli* strain W3110 in 1 L FM medium (20 g yeast extract, 8 g casamino acids, 1.55 g $MgSO_4$, 1 g sodium citrate, 0.2 g $CaCl_2$, 0.5 ml trace elements solution (36), 3 g NaH_2PO_4, 6 g K_2HPO_4) containing 1% glucose and 100 μg/ml ampicillin. Cells from overnight culture were collected by centrifugation (15 min, 5000 rpm, 25°C; Kontron, Zurich, Switzerland) and resuspended in the 4-fold volume of the overnight culture in FM medium + 100 μg/ml ampicillin without glucose. The culture was induced with 0.05 mM IPTG for 20 h at 25°C. After cell harvesting by centrifugation and preparation of periplasm by osmotic shock (30 min at 0°C in 200 mM sodium borate (pH 8.0), 160 mM NaCl, 10 mM EDTA), the scFv was present in both the soluble and the insoluble fraction.

Purification

For Ag affinity chromatography, a modified e-pep (affi-pep = GPGGGAT PQDLNTn; n = norleucine) was coupled to cyanogen bromide-activated Sepharose 4B (Pharmacia Biotec, Uppsala, Sweden). For Ag-independent affinity chromatography, biotinylated anti-myc tag mAb 9E10 was immobilized to streptavidin-Sepharose (Sigma, München, Germany). After filtration through a 0.2-μm membrane filter, the soluble fractions of periplasm and culture supernatant (the latter being concentrated 1:10 by ultrafiltration with a 10-kDa membrane) were directly applied to a 9E10 column equilibrated with 50 mM Tris-HCl (pH 8.0) and 150 mM NaCl. The column was first washed with the same buffer followed by a second wash with 50 mM Tris-HCl (pH 8.0), 1 M NaCl, and 1 mM EDTA, followed by a third wash step with 0.2 M glycine (pH 5.0) and 0.2 M NaCl. Homogeneous scFv fractions were eluted with 0.2 M glycine (pH 2.0) and 0.2 M NaCl and immediately neutralized with 2 M Tris-HCl, pH 9.0. After dialysis against PBS-buffer, scFv proteins were concentrated to 0.1–0.3 mg/ml by ultrafiltration using Centricon 10 concentrators (Amicon, Beverly, MA). All scFvs were characterized by SDS-PAGE, Western blot, and ELISA. In the Western blot analysis, a mixture of 2 μg/ml anti-myc tag mAb 9E10 (37) and 1:500 v/v HRP-labeled anti-mouse Ab (Amersham, Braunschweig, Germany) was used for specific detection of the CB4-1 scFvs.

The eluted scFvs were at least 95% pure as judged by SDS-PAGE and were used without further purification.

Site-directed mutagenesis

The site-directed mutagenesis was performed by the method of Deng and Nickoloff (38), which uses two primers, the first one introducing the mutation and the second one eliminating a unique selection site in the vector. The following mutation primers were used: V_H:Y^{32}A, 5′-Phos-CATAT TTACTGACGCTGAAATACAC; V_L:F^{94}A, 5′-Phos-CAGTATGATGA CGCTCCGCTCACGTTCGG;and V_L:P^{95}A, 5′-Phos-GTATGATGACTT TGCTCTCACGTTCGG. The following selection primer was used: Sca + Mlu-(pHEN), 5′-Phos-GACTTGGTTGACGCGTCACCAGTCACAG.

The resulting mutants were selected by restriction site analysis, ELISA screening, and Western blot analysis. Finally, the desired exchanges were confirmed by control sequencing.

Determination of binding constants: Fab competition ELISA

In the Fab competition ELISA, the HRP-labeled CB4-1 Fab competes with the Ab probe (Ab, Fab, and scFv) for binding to the native Ag p24 (HIV-1),

immobilized to the solid phase Microtiter plates (Nunc, Roskilde, Denmark) were coated with 0 1 μg/ml rp24 (39) in 0.1 M sodium carbonate buffer (pH 9.6) and incubated for 20 h at 4°C. After washing three times with PBS/0.1% Tween 20, 0.1 μg/ml HRP-labeled CB4-1 Fab was added with unlabeled mAb, Fab, or scFv in various concentrations (depending on the respective inhibition constants) in PBS/ 0.1% Tween 20 containing 6% Gelifundol S (Biotest, Dreieich, Germany) in a total volume of 50 μl for 20 h at 4°C. After washing three times with PBS/0.1% Tween 20, the bound enzymatic activity was determined by adding 5.5 mM *o*-phenylenediamine hydrochloride (Fluka, Buchs, Switzerland) and 8.5 mM H_2O_2 in 0.1 M citrate buffer (pH 5.0). The reaction was terminated after 10 min by adding 1 M sulfuric acid containing 0.05 M sodium sulfite. The absorbance was measured at 492 nm and as reference at 620 nm, using an ELISA reader (Anthos, Köln, Germany). Affinity constants were calculated according to Friguet et al. (40).

Determination of binding constants: peptide competition ELISA

For the peptide competition ELISA two kinds of solid-phase ligands were used to capture free Ab, Fab, or scFv. The first capture molecule was rp24, immobilized as described above. A second kind of capture molecule was N-terminally biotinylated peptides immobilized via streptavidin. Microtiter plates (Nunc) were coated with 5–0.5 μg/ml streptavidin (Sigma) in 0.1 M sodium carbonate buffer (pH 9.6) and incubated for 20 h at 4°C. After washing three times with PBS/0.1% Tween 20, 10 μg/ml biotinylated peptides were added in PBS/0.1% Tween 20 containing 6% Gelifundol S (Biotest) and incubated for 2 h at 25°C. After an additional three washes with PBS/0.1% Tween 20 decreasing amounts of peptides were mixed in a total volume of 50 μl with constant concentrations of the Ab, Fab, or scFv probe and incubated for 20 h at 4°C. CB4-1 mAb and Fab were detected with HRP-labeled anti-mouse Ab (1:500 v/v; Amersham) and scFv-fragments were detected with a mixture of the 1 μg/ml anti-myc tag mAb 9E10 (37) and 1:2000 v/v HRP-labeled anti-mouse Ab. After washing three times with PBS/0.1% Tween 20, the detection of bound enzymatic activity and calculation of affinity constants was performed as described above. Optimal concentrations for streptavidin coating of microtiter plates and for binding were selected by cross titration in direct binding assays.

Substitutional analysis of peptides

The peptides were synthesized on a β-Ala-β-Ala matrix bound to cellulose sheets at a spot according to Frank and Overwin (41) Each single position of the epitope was substituted by all other 19 amino acids resulting in the analysis of 209 epitope mutants.

The membrane-bound libraries were blocked overnight with blocking buffer (i.e., blocking reagent; Cambridge Research Biomedicals, Northwich, U.K.) in TBST containing 1% sucrose. After washing with, 1 μg/ml CB4-1 in blocking buffer was added and incubated for 3 h at room temperature. For the substitutional analyses, a concentration of 0.1 μg/ml scFv was applied. After three times washing with TBST, the anti-myc tag mAb 9E10 and a peroxidase-labeled anti-mouse Ab (Sigma; both Abs 1 μg/ml in blocking buffer) were applied for 2 h at room temperature For detection, a chemiluminescence system (Boehringer Mannheim) was applied using standard x-ray films. The relative spot intensities correlate with the binding affinities (42).

Structural modeling of the mutations

The modeling of the amino acid substitutions in the CB4-1 binding site was performed on the basis of the corresponding CB4-1 Fab/peptide x-ray structures (30). After the exchange of the mutated site chains using the modeling software Quanta (Micron Separations, San Diego, CA), a local energy minimization was performed with the CHARMm force field (Quanta) (43).

Results

Cloning, expression, and characterization of the scFv in E. coli

For a mutational analysis of the Ab binding region consisting of V_H and V_L, we cloned the corresponding scFv constructs with a $(Gly^4Ser)^3$Ala linker into the pHEN I vector, which includes the pelB signal peptide for periplasmic expression in *E. coli* and the myc tag as carboxy-terminal fusion peptide for affinity purification of the expression products (Fig. 1). The best yield was achieved with the *E. coli* strain W3110, cultured in a fermentation medium

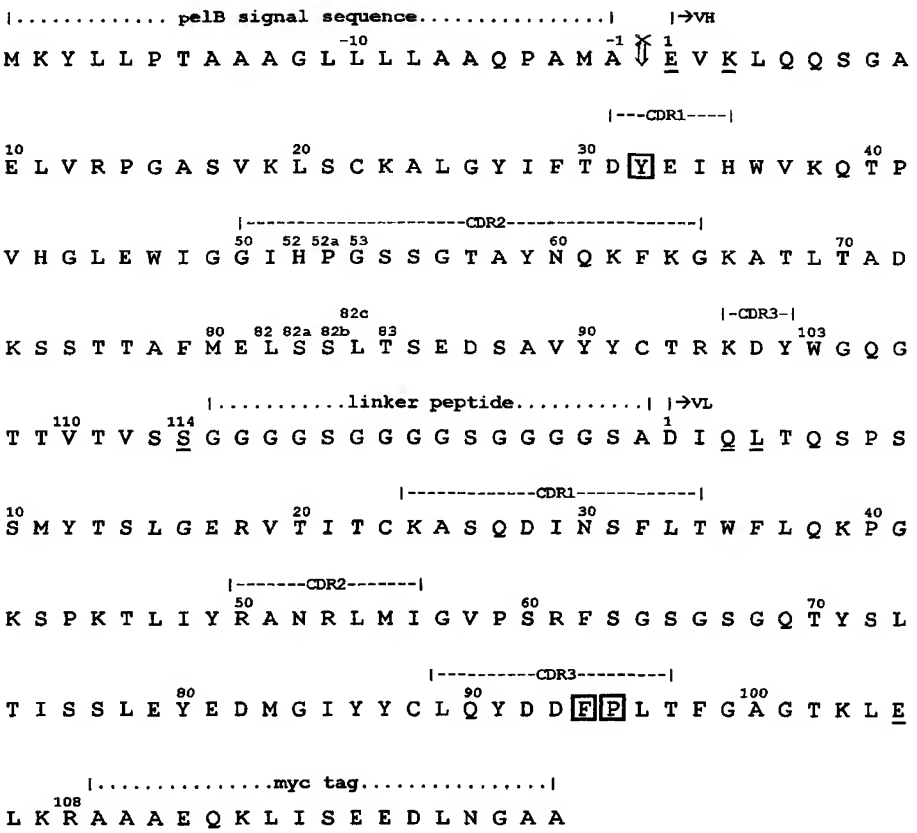

FIGURE 1. Amino acid sequence of the complete scFv CB4-1 with signal peptide and affinity tag. Numbering and CDR assignment according to Kabat et al. (44). ≻⇓, The cleavage site of the signal peptidase. Residues deviating from the original Ab sequence due to primer requirements are underlined. The three positions where mutations to Ala were introduced are boxed.

and induced with very low amounts of the inducer (0.05 mM IPTG). Following the optimized expression conditions described in *Materials and Methods*, usually 1–3 mg soluble CB4-1 scFv per liter cell culture were obtained.

Affinity chromatography was applied for purification of recombinant protein from soluble fractions of periplasm and culture supernatant using at the solid phase either a modified e-pep (affi-pep, for wild-type (wt) scFv) or the anti-myc tag mAb 9E10 (for mutant scFvs). Generally, fluorescence emission spectra of the mutants were inspected to assure that also the corresponding scFvs with low or lacking affinity are folded into the native conformation. Their emission spectra were not distinguishable from those of the wt scFv (data not shown). Furthermore, for wt scFv CB4-1 we know that on the one hand misfolded material is insoluble and that on the other hand there is no difference in affinity constants for soluble scFv batches independently, whether the affinity purification was performed using the anti-myc tag 9E10 Ab or an Ag peptide at the solid phase. Thus the copurification of substantial amounts of misfolded scFv material after affinity purification with anti-myc 9E10 can be excluded.

Fast protein liquid gel chromatography and ultracentrifugation revealed that the purified CB4-1 scFv is mainly dimeric (data not shown). The dimer-monomer ratio ranges from 70 to 90% depending on the expression and purification procedure applied.

The binding behavior of wt scFv-myc tag fragment was compared with that of the CB4-1 Fab and the complete mAb by two different competition ELISA experiments as shown in Fig. 2. The Fab competition assay (Fig. 2*A*) provides a measure of the avidity against the solid-phase Ag p24; the peptide competition assay (Fig. 2*B*) determines the affinity against the peptide in solution. The scFv of CB4-1 exhibits nearly the same binding behavior to p24 as the parental IgG Ab CB4-1, whereas the affinity of the Fab is significantly lower. This underlines the predominantly dimeric nature of the scFv. In contrast, the affinities of both scFv and Fab toward the e-pep are very similar to that of the mAb CB4-1 (Fig. 2*B*), which is to be expected because affinity constants derived from a competition assay should not be influenced by avidity effects. Therefore, the CB4-1 scFv expressed in *E. coli* is suitable for mutagenesis studies of the mAb CB4-1 binding region.

Mutagenesis of CB4-1 binding region

For mutational analysis of the Ab binding region, those amino acid side chains are of particular interest which potentially provide different contributions to the binding of the structurally unrelated peptides. By inspecting all CDR residues for which Ag contacts can be observed in the corresponding crystal structures of the two peptide/Fab complexes (30), and assisted by the results from the corresponding peptide substitutional analyses (31), such amino acids can be identified if they interact with a peptide key position in one peptide and with a nonkey position in the structurally unrelated peptide. The Ab residues V_H:Tyr^{32} and V_L:Phe^{94} are such residues, both in hydrophobic contact with the two unrelated peptides e-pep and epitope unrelated peptide (u-pep; Ref. 30). V_H:Tyr^{32} interacts with key positions in e-pep but not in u-pep, whereas it is vice versa with V_L:Phe^{94}. Nevertheless, those peptide residues identified as key positions must not necessarily reflect the

A

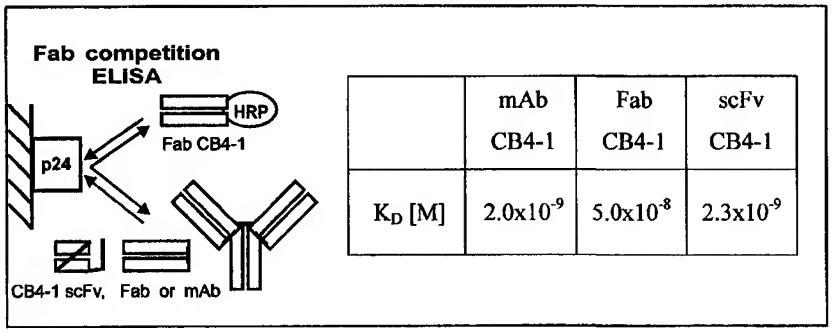

	mAb CB4-1	Fab CB4-1	scFv CB4-1
K_D [M]	2.0×10^{-9}	5.0×10^{-8}	2.3×10^{-9}

B

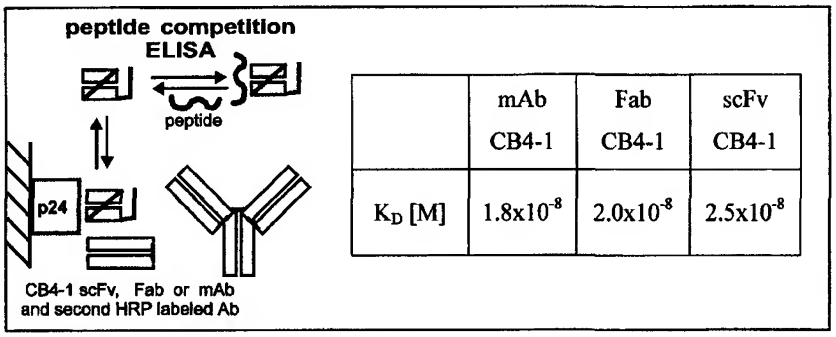

	mAb CB4-1	Fab CB4-1	scFv CB4-1
K_D [M]	1.8×10^{-8}	2.0×10^{-8}	2.5×10^{-8}

FIGURE 2. Affinity of the CB4-1 scFv to the Ag p24 (*A*) and to the e-pep GATPQDLNTnL (n = norleucine) (*B*) in comparison with CB4-1 mAb and the corresponding Fab, as measured by Fab competition ELISA (*A*) and by peptide competition ELISA (*B*). The principles of the two ELISA systems are presented schematically on the left.

importance of their interaction with individual residues in the Ag binding site, but may as well be the result of conformational restraints or requirements within the peptide (26). To investigate the binding contribution of V_H:Tyr^{32} and V_L:Phe^{94}, we substituted these residues with alanine. Additionally, we intended to check the influence of a noncontact CDR residue that is highly conserved in the germline-encoded κ light chain variable region genes. One of the most significant residues without direct Ag contact is the proline in position 95 of the light chain that stabilizes the CDRL3 loop in a conformation corresponding to the canonical structure 1 (8). In contrast, there is a structure reported for an anti-CD5 Ab which lacks this conserved proline in CDRL3, leading to a variant of the canonical structure (45). Thus, a mutation of this position in CB4-1 could show different influences on the binding of epitope related and nonrelated peptides. The V_L:Pro^{95} was again mutated to alanine.

The site-directed mutagenesis was performed by the method of Deng and Nickoloff (38) and the resulting mutants were selected by restriction site and Western blot analyses. Finally, the desired exchanges were confirmed by control sequencing for at least two mutant clones. After expression, the mutated scFv proteins were purified from the soluble fractions of periplasm and culture supernatant as described above.

Characterization of binding behavior of the scFv mutants

The binding behavior of wt and mutant scFvs of CB4-1 were compared by the two different ELISA mentioned above (see Fig. 2), using either the Fab of CB4-1 or the e-pep GATPQDLNTnL and the u-pep GLYEWGGARITNTD for scFv competition. The influence of the mutations on the binding of the natural Ag p24 is measured in the Fab competition ELISA (Fig. 3*A*). The alanine exchange of V_H:Tyr^{32} reduced the binding to immobilized p24 250-fold, that of V_L:Phe^{94} about 10-fold, and that of V_L:Pro^{95} to a nondetectable level ($K_D > 2 \times 10^{-4}$ M). Hence it follows that for the detection of free scFv mutants in the peptide competition ELISA it became necessary to modify the solid phase, because in competition assays, the solid phase requires high affinity to the captured molecule. Therefore, in parallel to p24 as the capturing molecule, we used biotinylated e-pep and u-pep which were immobilized on streptavidin-coated microtiter plates. In the cases where the peptide competition could be performed with both the biotinylated peptide and p24 as solid-phase Ag (scFv mutants V_H:Tyr^{32}Ala/u-pep and V_L:Phe^{94}Ala/e-pep), the values agree well, demonstrating the independence of the measured affinity on the nature of solid phase capturing molecule (data not shown). Peptide competition assays for the scFv mutants V_H:Tyr^{32}Ala with e-pep and for V_L:Phe^{94}Ala with u-pep can only be measured with biotinylated e-pep or u-pep at the solid phase. Because the affinity constants of wt CB4-1 to e-pep and u-pep differ by one order of magnitude (K_D [e-pep] = 1.3×10^{-8} M; K_D [u-pep] = 2.0×10^{-7} M) for better comparison of the values with respect to their mutational impact, the affinity constants are shown as relative affinity constants (rel.K_D = $K_D$scFv(wt)/$K_D$scFv(mutant)) in Fig. 3*B*. The influence of the mutations on the e-pep was completely the same as on the natural Ag p24 as measured in the Fab competition ELISA. For the u-pep, an opposite effect became obvious; whereas the mutation V_H:Tyr^{32}Ala results in an unchanged or even slightly enhanced binding, the affinity of the scFv mutant V_L:Phe^{94}Ala is 50-fold reduced. Thus, the single point mutation V_H:Tyr^{32}Ala causes a changed Ag binding specificity if taking into account the maintained u-pep binding and significantly reduced e-pep binding. The differing mutational effects were characterized in more detail by substitutional analysis of the two peptides with respect to the binding contribution of each amino acid residue in the peptides.

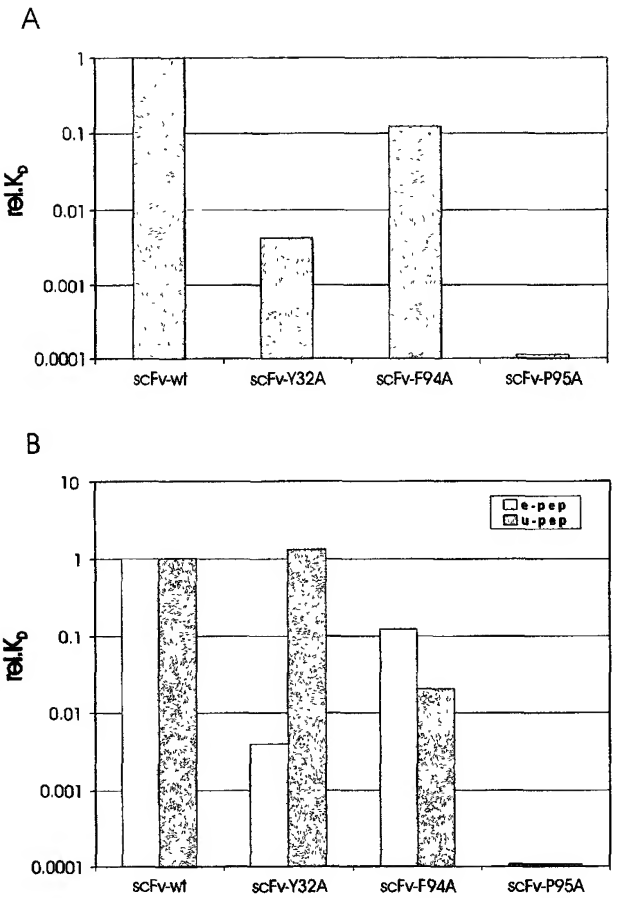

FIGURE 3. Influence of the scFv mutations on the binding of structurally unrelated Ags. The relative binding constants are calculated as rel.K_D = $K_D$scFv(wt)/$K_D$scFv(mutant). *A*, Changes in affinity to immobilized HIV-1 capsid protein p24 as measured in the Fab competition ELISA with p24 at the solid phase. *B*, Influence of the mutations on the binding of e-pep (GATPQDLNTnL) and u-pep (GLYEWGGARITNTD), as measured in the peptide competition ELISA.

Substitutional analyses with scFv mutants

In comparison to the wt scFv (Fig. 4*A*) the substitution matrix for the e-pep with scFv mutant V_H:Tyr^{32}Ala revealed a loss of selectivity in position proline 4 and a slightly increased selectivity in the positions alanine 2, aspartate 6, and asparagine 8 of the e-pep (Fig. 4*B*). Especially, the two latter residues cannot be substituted furthermore by any other amino acid. One new spot became visible in position 9 where the threonine can be substituted preferentially by aspartate which was not allowed for the wt scFv (Fig. 4, *A* and *B*). From inspection of the corresponding x-ray structure, it becomes evident that this aspartate may interact electrostatically with the heavy chain residue lysine 99. Similar to the V_H:Tyr^{32}Ala exchange, the scFv mutant V_L:Phe^{94}Ala displays with the e-pep substitution matrix an increased selectivity in the positions alanine 2, aspartate 6, and asparagine 8 (Fig. 4*C*). Opposite to the effect observed for the V_H:Tyr^{32}Ala mutation, the selectivity of the scFv mutant V_L:Phe^{94}Ala is additionally increased in position proline 4, whereas the selective binding in position methionine 10 is slightly decreased.

The substitution matrix of the u-pep with the scFv mutant V_H:Tyr^{32}Ala reveals an increased selectivity in comparison to the wt scFv (Fig. 4*D*) in the positions tryptophan 5, alanine 8, arginine 9, and isoleucine 10, as well as for the contact residue leucine 2 (Fig. 4*E*). Simultaneously, two increased signals in position 8 of the

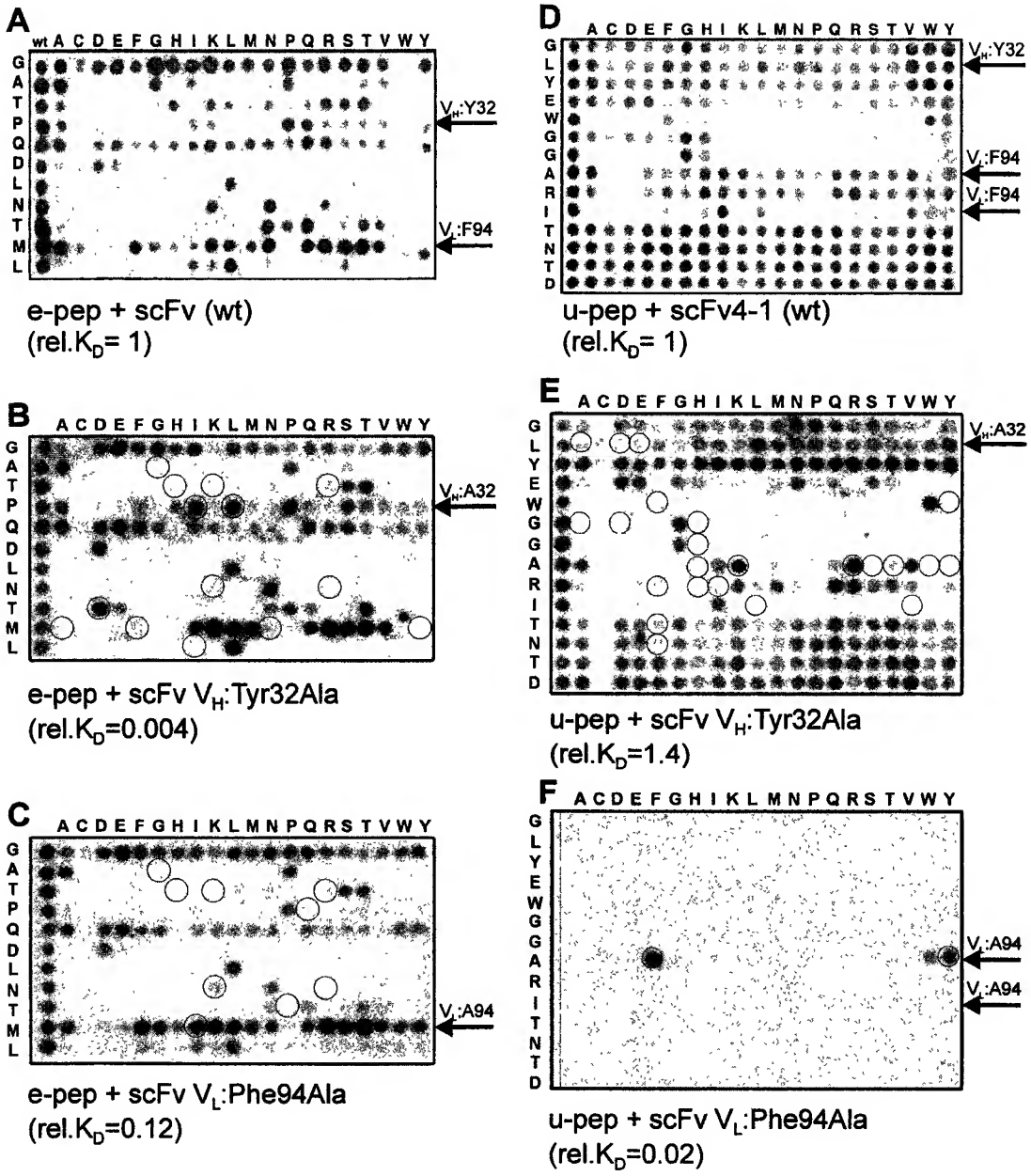

FIGURE 4. Binding patterns of wt scFv and mutant scFvs to complete substitutional matrices of e-pep and u-pep. *Left*, Peptides in the first row are identical and represent the starting peptides. Each position within the peptides was substituted by all amino acids (horizontal lines). Binding of scFvs to these single substitution analogues was visualized as described. For the mutants, the exposure time was elongated according the decreased affinity (rel.K_D is indicated below each array), with the exception of the u-pep substitution matrix and the V_L:Phe^{94}Ala mutant, where affinity restoring amino acid exchanges become visible during normal exposure time. The relative spot intensities correlate with the binding affinities. Arrows indicate positions where the mutated residues interact with peptide side chains as revealed by x-ray structure analysis (30). Circles around a spot mark positions where a significant new signal arises in comparison to the wt scFv. Circles without a spot mark positions where the binding signal disappeared (for a better overview, the empty circles were omitted in *F*).

u-pep indicate that the alanine can be preferentially exchanged against basic residues. In the corresponding x-ray structure there is the possibility that these positively charged side chains form a salt bridge with the carboxyl group of V_L:Asp^{93}. The substitutional analysis of u-pep with the scFv mutant V_L:Phe^{94}Ala (Fig. 4*F*) demonstrates that a single substitution, that of alanine 8 to phenylalanine, which is inverse to the mutation in the binding region, is able to restore the binding. The peptide with this compensatory substitution was called u-pep:Ala^{8}Phe and was synthesized as a soluble peptide for affinity measurements in solution.

Analysis of the u-pep:Ala^{8}Phe

The affinities of the wt and mutant scFvs to the peptide u-pep:Ala^{8}Phe were measured by peptide competition ELISA (Fig. 5). The affinity of the wt scFv to u-pep:Ala^{8}Phe is 1.3×10^{-6} M and, therefore, in the same order of magnitude as the affinity of the scFv mutant V_L:Phe^{94}Ala to u-pep ($K_D = 5.9 \times 10^{-6}$ M). In comparison to the wt scFv, the affinity of the V_H:Tyr^{32}Ala mutant to u-pep:Ala^{8}Phe is slightly decreased by a factor of about 4 ($K_D = 3.5 \times 10^{-6}$ M) whereas the affinity of the scFv mutant V_L:

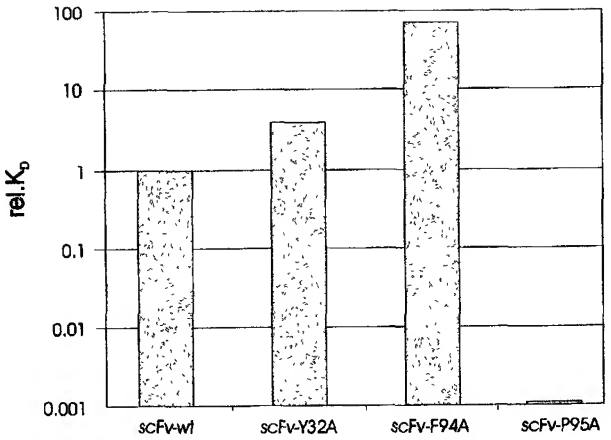

FIGURE 5. Influence of the scFv mutations on the binding of u-pep: Ala[8]Phe (GLYEWGGFRITNTD) as measured in the peptide-competition ELISA. The relative binding constants are calculated as rel.K_D = $K_D$scFv(*wt*)/$K_D$scFv(*mutant*).

Phe[94]Ala was increased 80-fold to a K_D of 1.6×10^{-8} M. This increase not only restores the binding of the mutant scFv to u-pep: Ala[8]Phe, but it results in a nearly 10-fold higher affinity than the original wt scFv/u-pep interaction, thus increasing the affinity of u-pep-Ala[8]Phe to the value of the e-pep/wt scFv interaction. As a result, the preferential binding of wt scFv to e-pep has switched for the scFv mutant V_L:Phe[94]Ala, which shows the highest affinity to u-pep: Ala[8]Phe, whereas e-pep binding is discriminated by the factor of 80.

Discussion

Polyreactivity and germline genes

Polyreactive Abs, which are frequently also designated as NAA in the literature, form a substantial part of the normal B cell repertoire (1, 2). A characteristic shared by many of these Abs is their binding to various dissimilar Ags such as proteins, nucleic acids, and polysaccharides (5, 46, 47). This broad specificity may be responsible for a major role of these kinds of Abs in primary defense against invading agents before higher specific Abs are produced by the immune system (2). It has been found that similar V genes can encode both natural poly/autoreactive and Ag-induced Abs (48). However, the most significant difference between NAA and Ag-induced Abs from normal immune response is that NAA do not undergo Ag-dependent affinity maturation, their variable regions being always in a close germline configuration (5, 49, 50). In contrast to this, an Ag-induced Ab passes through multiple rounds of somatic hypermutation and selection in germinal centers. With respect to the polyspecific binding capability of the CB4-1, the question arises whether the variable region sequences of mAb CB4-1 are nearly identical with germline-encoded V genes, which would point to a "natural" polyreactivity, or whether they show typical features of somatic hypermutation normally found in T cell-dependent affinity maturation. To address this, we performed multiple sequence alignments with known putative germline V genes.[4] Inspecting the somatic mutations of CB4-1 V_H and V_L with respect to the number of mutations, the hot spots, the frequency of transitions vs transversions, and the N-region addition, they show all typical features of an Ag-dependent affinity maturation with multiple rounds of diversification and selection (51, 52) Therefore, despite its polyspecific binding behavior toward a number of nonhomologous peptides, the mAb CB4-1 can be considered a normal Ag-specific Ab. This is to be expected because the Ab was derived from secondary immune response after repeated administration of the Ag HIV-1 capsid protein p24 (28).

Cloning, expression, and characterization of the scFv

Cloning and expression of the variable region of Abs as an scFv in *E. coli* is a widely used method to exploit the specific binding capacity of a certain Ab and offers the possibility to use site-directed mutagenesis to investigate the binding contribution of distinct amino acid residues (53–56). The binding behavior of wt scFv CB4-1 was characterized by two different competition ELISA experiments. The Fab competition ELISA measures the affinity (or avidity) to the solid-phase immobilized rp24. Ligands with two binding sites can bind the solid phase adsorbed Ag with a higher functional affinity (avidity). This is the reason for the lower K_D values of the mAb and the mainly dimeric wt scFv as compared with the corresponding Fab in the Fab competition ELISA (Fig. 2*A*). The peptide competition ELISA determines the binding constant for the peptides in solution. We obtained no significant differences in the K_D values between complete mAb and its fragments in the peptide competition ELISA. This is supported by earlier comparisons of fluorescence quenching measurements with peptides in solution, and peptide ELISA (29). Therefore, there was no need to analyze the dimer-monomer ratio for the mutated scFvs as well. Taken together, despite the primer-encoded differences in the terminal sequences of framework region 1 or framework region 4 in comparison with the original V_H and V_L sequences, the scFv of CB4-1 exhibits the same affinity as the parental Ab indicating that these sequence deviations, the fragmentation, the dimerization, or the myc tag fusion do not influence the binding behavior at all.

Mutation of the CB4-1 binding site

Usually, the polyreactivity of germline-encoded Abs is structurally accomplished by a higher flexibility which allows the binding of a wide range of Ags, but with low affinity (4). Somatic mutations introduced into the hypervariable CDR loops (but also sometimes into adjacent framework residues) during Ag-dependent affinity maturation result in a combining site with improved complementarity to the Ag which in contrast to the germline-derived Ab binds the Ag in a preorganized fashion. In addition to enthalpic effects, entropic restriction of residues in the combining site plays a key role in the increase of binding affinity (4). Nevertheless, a limited number of molecules which may be structurally related (crossreactivity) or unrelated (polyreactivity) can fit with high affinity in a more rigid binding site of affinity maturated Abs (22–24, 30). In the case of CB4-1, the conformation and binding mode of the u-pep drastically differ from the e-pep (30). The contribution of single amino acid residues to the binding energy cannot be derived easily from crystal structure analysis but can be revealed by substitutional analysis of the peptide itself (31) and by mutagenesis experiments at the Ab binding site (13, 18). For the latter case usually alanine exchange was chosen because it minimizes the side chain without altering the main-chain conformation and does not impose extreme steric or electrostatic effects.

The measurement of the K_D values by competition ELISA displays decreases in affinity to the peptides by factors in the range from 10 to 1000 for the CB4-1 scFv mutants. The strongest effect was obtained for the alanine mutation of the canonical residue V_L:Pro[95] which is not in contact with the corresponding peptides.

[4] It has to be mentioned that not all murine germline genes are sequenced so far. A possible way to complete the sequence information is the delineation of a consensus sequence deduced from rearranged V genes with the highest homology Following this strategy, we identified a cluster of four sequences (MMMAMST2, MMU09596, MMU09502, and S73896) with a consensus sequence which is probably germline encoded (data not shown).

In reasons of maintained native folding of the mutated scFv proteins as revealed by an unchanged fluorescence emission spectra, the alanine mutation of V_L:Pro^{95} obviously results in a conformational change of the light chain CDR3 which is unfavorable for both e-pep and u-pep binding despite that this CDR exhibits much more critical contacts with u-pep than with e-pep (30). Thus, this may point to some functional cooperativity between different CDRs within the binding site. Nevertheless, despite that this Pro^{95} is largely conserved between Ab κ-chains, this does not necessarily mean that an exchange of proline at this position generally leads to a loss in Ag affinity, as it is seen with an anti-CD5 Ab which lacks this conserved proline in CDRL3 (33).

The structurally unrelated peptides e-pep and u-pep interact with different sets of peptide residues to a similar set of amino acid side chains in the Ab binding region. Crystal structure analysis of the CB4-1 peptide/Fab complexes displays for the V_H:Tyr^{32} residue hydrophobic contacts to e-pep proline 4 and to u-pep leucine 2. For the latter, the x-ray data show extensive hydrophobic stacking with u-pep tryptophane 5 and CB4-1 V_L:Tyr^{49} (Fig. 6). Additionally, a hydrogen bound for e-pep was observed between V_H:Tyr^{32} and the carbonyl oxygen of alanine 2. Despite that both peptides exhibit distinct hydrophobic contacts to the V_H:Tyr^{32} in the unmutated binding region, the scFv mutant V_H:Tyr^{32}Ala displays a 250-fold reduced binding to the e-pep, whereas the binding to u-pep remains unchanged. Modeling of alanine substitution of V_H:Tyr^{32} shows that there is no side chain orientation for Leu^2 which allows a reconstitution of the u-pep:Leu^2/V_H:Ala^{32} contact (Fig. 6). Hence, it must be concluded that the wt Leu^2/V_H:Tyr^{32} contact does not contribute much to the free energy of u-pep binding. This is supported by the substitutional analysis of u-pep with wt scFv which demonstrates that leucine 2 can be substituted by all other residues (Fig. 4*D*). In contrast, the loss of the contact with the "key residue" Ile10 for the V_H:Phe^{94}Ala mutant leads to a drastic decrease in affinity, affirming that this key position indeed reflects a thermodynamically important residue interaction. The same conclusion can be drawn for the behavior of the mutants toward e-pep; there is much more loss of affinity for the V_H:Tyr^{32}Ala mutant without the contact to the key residue Pro^4 than for the VL:Phe^{94}Ala mutant without the contact to the nonkey residue Met^{10}.

Generally, substitutional analyses of peptides where each position of the peptides is substituted by all 19 other amino acids is a powerful method to analyze how mutations in the Ab combining site can change the preferentially interacting key residues of Ags in the context of polyspecificity (31). The less amino acid substitutions are accepted in a certain position the more stringent are the sterical and energetical constraints for maintaining the Ab binding, thus reflected by an increased selectivity in that position. For the whole range of potential ligand molecules an increased selectivity would result in a smaller ensemble of binding peptides, which means an increased Ab specificity.

The analysis of the u-pep substitution matrix incubated with scFv mutant V_H:Tyr^{32}Ala reveals that changes in position-specific binding patterns occur not only in the contact position leucine 2 (and tryptophane 5, which is involved in a hydrophobic stack with

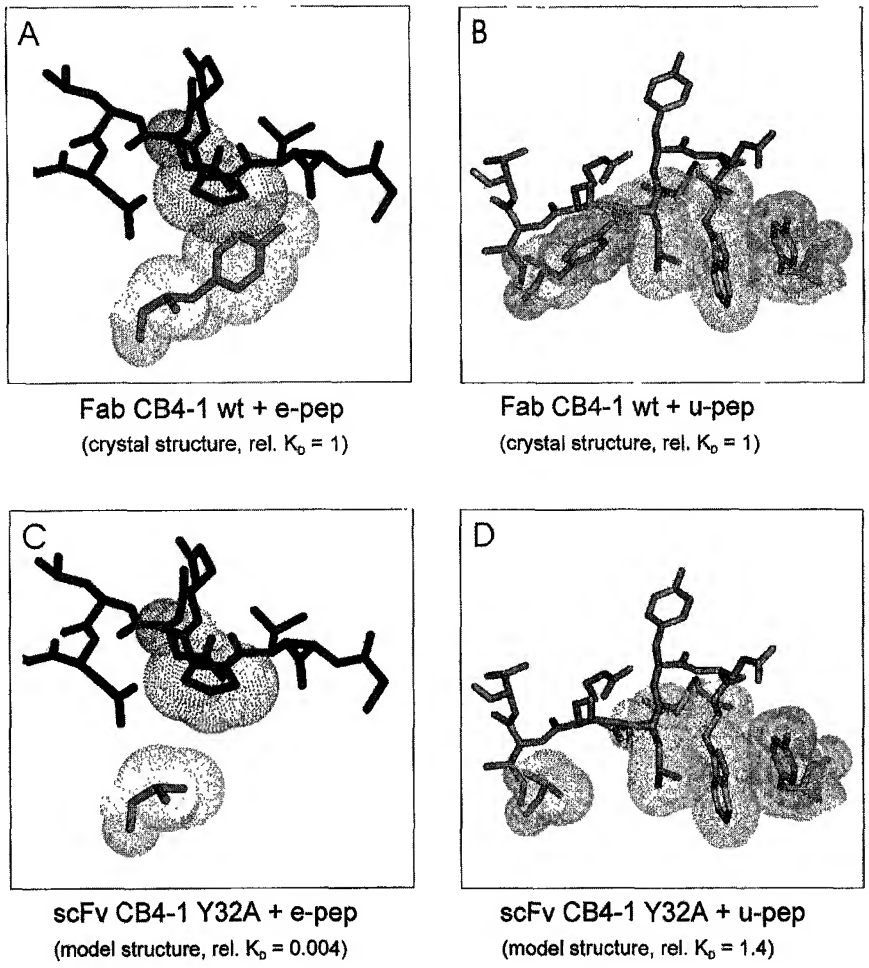

FIGURE 6. Structural consequences of V_H:Tyr^{32}Ala mutation and their influences on the binding of e-pep (red) or u-pep (blue). Residues from the Ab are in green; interaction between V_H:Tyr^{32} and e-pep (*A*) or u-pep (*B*) as seen in the crystal structure, and mutation V_H:Ala^{32} demonstrating the loss of van-der-Waals contacts to e-pep (*C*) and u-pep (*D*). The rel.K_D given reflect the changes in binding constants in comparison to the binding of the unmutated scFv as measured with the peptide competition ELISA. Modeling and representation of the mutation was generated using Quanta software.

Leu[2]. Fig. 6). As illustrated in Fig. 4, changes in the substitution pattern are obvious in nearly all positions of u-pep. Similar effects were observed for the other peptide-scFv mutant combinations as well. In general, the selective binding is reduced in contact positions and increased in all noncontact positions. From this it may be concluded that independently of the affinity changes small rearrangements over the whole peptide are necessary to compensate the structural alterations caused by the mutation. Comparably complex structural changes are described for the affinity maturation of the Ab combining site for the catalytic Ab 48G7 (57).

For the scFv mutant V_L:Phe[94]Ala, the substitutional analysis of u-pep reveals the inverse compensatory peptide mutation Ala[8]Phe. Fig. 7 illustrates the structural changes which are responsible for the observed effect. The modeled structure shows that there is free space now around the side chain of V_L:Ala[94], so that large hydrophobic side chains can now be accepted in the corresponding peptide contact position without sterical hindrance (Fig. 4*F*). The affinity of u-pep:Ala[8]Phe to the scFv mutant V_L:Phe[94]Ala is not only restored, but it is increased up to the range of that for the e-pep/wt scFv interaction.

Considering that mutations during the process of hypermutation will be introduced randomly and thereafter selected via receptor engagement (Ag affinity), our results thus represent an experimental example for the possibility of affinity maturation in the absence of a target (auto) Ag. This becomes obvious if one compares the affinity of the V_L:Phe[94]Ala mutation to u-pep:Ala[8]Phe with that to the native Ag, e-pep.

General conclusions

Single amino acid substitutions in an Ab binding region can change the specific binding of a certain functional epitope by two orders of magnitude or even more, as seen for other examples (57). At the same time, the affinity to another functional epitope may remain unchanged or even be increased. This results in a switch of

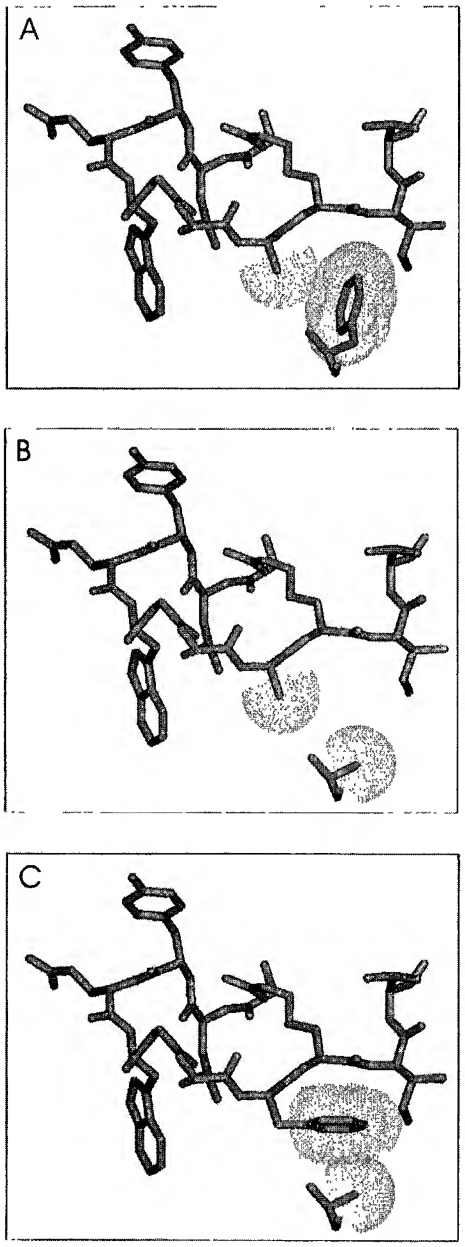

FIGURE 7. Influence of V_L:Phe[94]Ala mutation on the hydrophobic interaction with u-pep or u-pep:Ala[8]Phe. *A*, Van-der-Waals contact between V_L:Phe[94] (green) and u-pep: Ala[8] (blue) as seen in the crystal structure. *B*, Loss of the contact between the mutated light chain residue Ala[94] (green) and u-pep:Ala[8] (blue). *C*, Restored interaction between V_L: Ala[94] (green) and the substituted u-pep: Ala[8]Phe (blue). The rel.K_D given reflect the changes in binding constants in comparison to the binding of the unmutated scFv as measured by the peptide competition ELISA. Modeling and representation of the mutation was generated using Quanta software.

the preferentially bound Ag and therefore, represents a change in Ag binding specificity. On the one hand, from the immunological point of view this means that each time when an affinity maturated B cell introduces a new somatic mutation a possible autoreactive specificity can arise. This may be the initial step for the proliferation of an autoimmune B cell clone. On the other hand, for Abs used in therapy, such selective change of Ag binding specificity offers the possibility of reducing a harmful side specificity against self Ags, but without changing the desired target binding specificity, just by introducing single point mutations.

Acknowledgments

We thank Dr. G. Grütz for advice and critical reading of the manuscript; C. Landgraf, B. Hoffmann, and M. Affeldt for peptide synthesis; and H. Tanzmann for CB4-1 Ab preparations

References

1. Dighiero, G., B. Guilbert, and S. Avrameas. 1982 Naturally occurring antibodies against nine common antigens in humans sera. II. High incidence of monoclonal Ig exhibiting antibody activity against actin and tubulin and sharing antibody specificities with natural antibodies. *J Immunol. 128 2788.*
2. Guilbert, B., G. Dighiero, and S. Avrameas. 1982. Naturally occurring antibodies against nine common antigens in human sera I. Detection, isolation and characterization. *J. Immunol 128 2779*
3. Kelsoe, G. 1996. The germinal center a crucible for lymphocyte selection *Semin Immunol. 8 179.*
4. Wedemayer, G. J., P A. Patten, L H Wang, P. G. Schultz, and R. C Stevens. 1997. Structural insights into the evolution of an antibody combining site *Science 276 1665.*
5. Coutinho, A , M D. Kazatchkine, and S. Avrameas. 1995 Natural autoantibodies. *Curr. Opin. Immunol 7·812*
6. Padlan, E A 1994. Anatomy of the antibody molecule. *Mol Immunol 31 169.*
7. Chothia, C , and A M. Lesk 1987 Canonical structures for the hypervariable regions of immunoglobulins. *J Mol Biol 196 901.*
8. Al Lazikani, B., A M Lesk, and C. Chothia. 1997. Standard conformations for the canonical structures of immunoglobulins. *J. Mol. Biol. 273 927.*
9. Padlan, E A., C Abergel, and J. P. Tipper. 1995. Identification of specificity-determining residues in antibodies. *FASEB J. 9 133*
10. Webster, D M., A. H. Henry, and A. R. Rees. 1994. Antibody-antigen interactions *Curr Opin Struct Biol 4 123*
11. Wilson, I. A , and R L Stanfield 1993. Antibody-antigen interactions *Curr Opin Struct Biol 3:113.*
12. Brummell, D. A., V. P. Sharma, N N Anand, D. Bilous, G. Dubuc, J. Michniewicz, C. R Mackenzie, J Sadowska, B. W. Sigurskjold, B. Sinnott, et al 1993 Probing the combining site of an anti-carbohydrate antibody by saturation-mutagenesis· role of the heavy-chain CDR3 residues *Biochemistry 32 1180*
13. Dall'Acqua, W., E. R Goldman, E Eisenstein, and R. A Mariuzza 1996 A mutational analysis of the binding of two different proteins to the same antibody *Biochemistry 35 9667*
14 Near, R. I., M. Mudgett Hunter, J Novotny, R. Bruccoleri, and S C. Ng 1993. Characterization of an anti-digoxin antibody binding site by site-directed in vitro mutagenesis. *Mol Immunol. 30 369*
15 Hawkins, R E , S. J. Russell, M Baier, and G. Winter 1993 The contribution of contact and noncontact residues of antibody in the affinity of binding to antigen· the interaction of mutant D1.3 antibodies with lysozyme *J Mol. Biol 234 958*
16 Schier, R , R. F Balint, A McCall, G. Apell, J. W. Larrik, and J. D Marks 1996. Identification of functional and structural amino-acid residues by parsimonious mutagenesis. *Gene 169 147.*
17 Glockshuber, R , J. Stadlmuller, and A Pluckthun 1991. Mapping and modification of an antibody hapten binding site. a site-directed mutagenesis study of McPC603. *Biochemistry 30 3049*
18. Kelley, R F., and M P. Oconnell. 1993 Thermodynamic analysis of an antibody functional epitope. *Biochemistry 32.6828*
19. Braden, B. C , and R. J Poljak. 1995 Structural features of the reactions between antibodies and protein antigens. *FASEB J 9 9.*
20. Tello, D , F. A Goldbaum, R. A Mariuzza, X Ysern, F. P. Schwarz, and R. J Poljak. 1993 3-Dimensional structure and thermodynamics of antigen binding by antilysozyme antibodies. *Biochem. Soc Trans 21:943.*
21. Ito, W , Y. Iba, and Y. Kurosawa 1993. Effects of substitutions of closely related amino acids at the contact surface in an antigen-antibody complex on thermodynamic parameters. *J Biol Chem 268:16639.*
22 Pinilla, C., S. Chendra, J. R Appel, and R. A. Houghten 1995. Elucidation of monoclonal antibody polyspecificity using a synthetic combinatorial library *Pept Res. 8 250.*
23 Appel, J R., J. Buencamino, R. A Houghten, and C Pinilla 1996. Exploring antibody polyspecificity using synthetic combinatorial libraries *Mol Divers. 2 29.*
24. Kramer, A , T. Keitel, K. Winkler, W. Stocklein, W. Hohne, and J SchneiderMergener. 1997 Molecular basis for the binding promiscuity of an anti-p24 (HIV-1) monoclonal antibody. *Cell 91:799*
25. Arevalo, J. H., M. J. Taussig, and I. A. Wilson. 1993. Molecular basis of cross-reactivity and the limits of antibody antigen complementarity. *Nature 365:859.*
26 Arevalo, J H , E A Stura, M J Taussig, and I A Wilson 1993 3-Dimensional structure of an anti-steroid Fab' and progesterone Fab' complex *J. Mol Biol 231 103*
27 Berneman, A , B. Guilbert, S Eschrich, and S Avrameas 1993 IgG auto and polyreactivities of normal human sera *Mol Immunol 30 1499*
28 Grunow, R., R Giese, T Porstmann, H Döpel, K Hansel, and R von Baehr 1990 Development and biological testing of human and murine monoclonal antibodies against HIV antigens *Z Klin Med 45 367*
29 Hohne, W , G Kuttner, S Kiessig, G Hausdorf, G Grunow, K Winkler, H. Wessner, E. Giessmann, J Schneider, R von Baehr, and D Schomburg. 1993. Structural base of the interaction of a monoclonal antibody against p24 of HIV-1 with its peptide epitope *Mol Immunol 30 1213*
30. Keitel, T , A. Kramer, H. Wessner, C. Scholz, J Schneider-Mergener, and W Hohne. 1997. Crystallographic analysis of anti-p24 (HIV-1) monoclonal antibody cross-reactivity and polyspecificity *Cell 91:811*
31 Schneider-Mergener, J , A Kramer, and U Reineke 1996 Peptide libraries bound to continuous cellulose membranes tools to study molecular recognition In *Combinatorial Libraries* R Cortese, ed de Gruyter, Berlin, p. 53.
32 Küttner, G , E. Giessmann, B. Niemann, K. Winkler, R. Grunow, J Hinkula, J. Rosen, B Wahren, and R. von Baehr. 1992 Fv sequence and epitope mapping of a murine monoclonal antibody against p24 core protein of HIV-1 *Mol Immunol. 29 561.*
33 Jones, S T , and M M. Bendig. 1991. Rapid PCR-cloning of full-length mouse immunoglobulin variable regions *Bio/Technology 9.88.*
34 Orlandi, R., D H. Güssow, P. T. Jones, and G Winter. 1989. Cloning immunoglobulin variable domains for expression by the polymerase chain reaction. *Proc Natl Acad Sci USA 86 3833.*
35. Hoogenboom, H R., A D. Griffiths, K. S. Johnson, D J Chiswell, P. Hudson, and G. Winter 1991. Multi-subunit proteins on the surface of filamentous phage methodologies for displaying antibody (Fab) heavy and light chains. *Nucleic Acids. Res. 19 4133.*
36. Kleman, G L , J J. Chalmers, G. W. Luli, and W R Strohl. 1991. A predictive and feedback control algorithm maintains a constant glucose concentration in fed-batch fermentations. *Appl Environ Microbiol. 57 910.*
37 Evan, G I , G. K Lewis, G. Ramsay, and J. M. Bishop 1985. Isolation of monoclonal antibodies specific for human c-*myc* proto-oncogene product. *Mol Cell Biol 5 3610*
38. Deng, W P , and J. A Nickoloff 1992. Site-directed mutagenesis of virtually any plasmid by eliminating a unique site. *Anal Biochem. 200 81.*
39 Hausdorf, G , A. Gewiess, V. Wray, and T. Porstmann 1994. A recombinant human immunodeficiency virus type-1 capsid protein (rp24): its expression, purification and physico-chemical characterization *J. Virol Methods 50 1.*
40 Friguet, B , A F Chaffotte, L Djavadi Ohaniance, and M E Goldberg. 1985 Measurement of the true affinity constant in solution of antigen-antibody complexes by enzyme-linked immunosorbent assay. *J Immunol Methods 77 305.*
41 Frank, R., and H. Overwin. 1996. Spot synthesis In *Epitope Mapping Protocols.* G. E. Morris, ed. Humana Press, Totowa, p. 149
42. Volkmer-Engert, R., B Ehrhard, J. Hellwig, A. Kramer, W. E. Hohne, and J. Schneider-Mergener. 1994. Preparation, analysis and antibody binding studies of simultaneously synthesized soluble and cellulose-bound HIV-1 p24 peptide epitope libraries. *Lett Pept. Sci 1 243.*
43 Brooks, B. R., R. E. Bruccoleri, B. D. Olafsen, D. J States, S Swaminathan, and M Karplus. 1983. CHARMm. a program for macromolecular energy, minimization and dynamics calculation *J Comput Chem 4 187*
44 Kabat, E A , T T Wu, H. M Perry, K S Gottesman, and C. Foeller. 1991. *Sequences of Proteins of Immunological Interest*, 5th Ed., Public Health Service, National Institutes of Health, Cambridge.
45 Guarne, A., J. Bravo, J Calvo, F Lozano, J. Vives, and I. Fita 1996 Conformation of the hypervariable region L3 without the key proline residue. *Protein Sci 5:167*
46. Thompson, K. M , J. Sutherland, G. Barden, M. D. Melamed, M G Wright, S Bailey, and S J. Thorpe. 1992. Human monoclonal antibodies specific for blood group antigens demonstrate multispecific properties characteristic of natural autoantibodies. *Immunology 76 146.*
47. Puccetti, A , M. P. Madaio, G. Bellese, and P Migliorini 1995. Anti-DNA antibodies bind to DNase I *J Exp Med 181 1797*
48 Bona, C. A 1988 V genes encoding autoantibodies. molecular and phenotypic characteristics *Annu Rev. Immunol 6 327*
49. Diaw, L , C Magnac, O Pritsch, M. Buckle, P. M. Alzari, and G Dighiero 1997. Structural and affinity studies of IgM polyreactive natural autoantibodies *J. Immunol. 158:968.*
50. Logtenberg, T., M. E M Schutte, S B. Ebeling, F H J. Gmelig-Meyling, and J H van Es 1992 Molecular approaches to the study of human B-cell and (auto)antibody repertoire generation and selection. *Immunol Rev 128·23*
51. Wiesendanger, M., M D. Scharff, and W Edelmann 1998. Somatic hypermutation, transcription, and DNA mismatch repair. *Cell 94·415.*
52 Berek, C. 1993 Somatic mutation and memory. *Curr Opin Immunol 5 218.*
53 Sharon, J., C. Y. Kao, and S. R. Sompuram. 1993 Oligonucleotide-directed mutagenesis of antibody combining sites *Int Rev Immunol. 10 113*
54. Denzin, L. K., G. A. Gulliver, and E W. Voss Jr 1993. Mutational analysis of active site contact residues in anti-fluorescein monoclonal antibody 4-4-20. *Mol Immunol 30 1331*
55 Dougan, D A , R L Malby, L. C. Gruen, A. A. Kortt, and P J. Hudson 1998 Effects of substitutions in the binding surface of an antibody on antigen affinity. *Protein Eng. 11 65.*
56. Parhami, S B., and M. N Margolies. 1996. Contribution of heavy chain junctional amino acid diversity to antibody affinity among *p*-azophenylarsonate-specific antibodies. *J. Immunol 157 2066.*
57. Patten, P A , N S Gray, P L Yang, C. B. Marks, G J. Wedemayer, J. J. Boniface, R C. Stevens, and P. G. Schultz 1996 The immunological evolution of catalysis. *Science 271 1086.*

Protein Science (1994), *3*:737–749. Cambridge University Press. Printed in the USA.

Contribution of a single heavy chain residue to specificity of an anti-digoxin monoclonal antibody

JOEL F. SCHILDBACH,[1,7] SHYH-YU SHAW,[2,8] ROBERT E. BRUCCOLERI,[4] EDGAR HABER,[5] LEONARD A. HERZENBERG,[6] GINA C. JAGER,[6] PHILIP D. JEFFREY,[4,9] DAVID J. PANKA,[2,10] DAVID R. PARKS,[6] RICHARD I. NEAR,[2] JIRI NOVOTNY,[4] STEVEN SHERIFF,[4] AND MICHAEL N. MARGOLIES[2,3]

[1] Program on Immunology, Harvard University Graduate School of Arts and Sciences, Cambridge, Massachusetts 02138
[2] Department of Medicine and [3] Department of Surgery, Massachusetts General Hospital and Harvard Medical School, Boston, Massachusetts 02114
[4] Bristol-Myers Squibb Pharmaceutical Research Institute, Princeton, New Jersey 08543
[5] Cardiovascular Biology Laboratory, Division of Biological Sciences, Harvard School of Public Health, Boston, Massachusetts 02115
[6] Department of Genetics, Stanford University, Stanford, California 94305

(RECEIVED September 29, 1993; ACCEPTED February 9, 1994)

Abstract

Two distinct spontaneous variants of the murine anti-digoxin hybridoma 26-10 were isolated by fluorescence-activated cell sorting for reduced affinity of surface antibody for antigen. Nucleotide and partial amino acid sequencing of the variant antibody variable regions revealed that 1 variant had a single amino acid substitution: Lys for Asn at heavy chain position 35. The second variant antibody had 2 heavy chain substitutions: Tyr for Asn at position 35, and Met for Arg at position 38. Mutagenesis experiments confirmed that the position 35 substitutions were solely responsible for the markedly reduced affinity of both variant antibodies. Several mutants with more conservative position 35 substitutions were engineered to ascertain the contribution of Asn 35 to the binding of digoxin to antibody 26-10. Replacement of Asn with Gln reduced affinity for digoxin 10-fold relative to the wild-type antibody, but maintained wild-type fine specificity for cardiac glycoside analogues. All other substitutions (Val, Thr, Leu, Ala, and Asp) reduced affinity by at least 90-fold and caused distinct shifts in fine specificity. The Ala mutant demonstrated greatly increased relative affinities for 16-acetylated haptens and haptens with a saturated lactone.

The X-ray crystal structure of the 26-10 Fab in complex with digoxin (Jeffrey PD et al., 1993, *Proc Natl Acad Sci USA 90*:10310–10314) reveals that the position 35 Asn contacts hapten and forms hydrogen bonds with 2 other contact residues. The reductions in affinity of the position 35 mutants for digoxin are greater than expected based upon the small hapten contact area provided by the wild-type Asn. We therefore performed molecular modeling experiments which suggested that substitution of Gln or Asp can maintain these hydrogen bonds whereas the other substituted side chains cannot. The altered binding of the Asp mutant may be due to the introduction of a negative charge. The similarities in binding of the wild-type and Gln-mutant antibodies, however, suggest that these hydrogen bonds are important for maintaining the architecture of the binding site and therefore the affinity and specificity of this antibody. The Ala mutant eliminates the wild-type hydrogen bonding, and molecular modeling suggests that the reduced side-chain volume also provides space that can accommodate a congener with a 16-acetyl group or saturated lactone, accounting for the altered fine specificity of this antibody.

Keywords: anti-digoxin antibody; complementarity; fluorescence-activated cell sorting; hapten docking; hybridoma variant

Reprint requests to: Michael N. Margolies, Jackson 14, Massachusetts General Hospital, Boston, Massachusetts 02114; e-mail: frost@helix.mgh.harvard.edu.

[7] Present address: Department of Biology, Massachusetts Institute of Technology, Cambridge, Massachusetts 02139.

[8] Present address: Bristol-Myers Squibb Pharmaceutical Research Institute, Princeton, New Jersey 08543.

[9] Present address: Department of Cellular Biochemistry and Biophysics, Memorial Sloan-Kettering Cancer Center, New York, New York 10021.

[10] Present address: Department of Microbiology, Boston University School of Medicine, Boston, Massachusetts 02118.

The X-ray crystal structures of antibodies complexed with antigen or hapten (Amit et al., 1986; Sheriff et al., 1987b; Herron et al., 1989; Padlan et al., 1989; Alzari et al., 1990; Bentley et al., 1990; Fischmann et al., 1990; Stanfield et al., 1990; Brunger et al., 1991; Cygler et al., 1991; Rini et al., 1992; Tulip et al., 1992; Arevalo et al., 1993; Rose et al., 1993; Vix et al., 1993) suggest that the specificity of antibody recognition is reliant upon a high degree of complementarity between the antigen-combining site and antigen. The surfaces of the antibody and antigen often fit together with enough precision to exclude most

water molecules from the interface. The complementarity also extends to the precise positioning of atoms to allow charge-charge interactions and hydrogen bond formation between antibody and antigen. Although it then follows that altering the structure of the binding site will affect recognition, it has proven difficult to predict how a particular amino acid substitution will modulate antibody specificity.

To correlate antibody sequence with binding function, we are studying high-affinity anti-digoxin monoclonal antibodies (Mudgett-Hunter et al., 1982). We previously described variants of anti-digoxin hybridoma cell lines that secrete antibody possessing altered hapten binding due to variable (V) region substitutions (Panka et al., 1988; Schildbach et al., 1991). Here we detail the isolation of 2 V region variants of the anti-digoxin hybridoma 26-10. Each variant produced antibody with drastically reduced affinity for digoxin, due to 1 or 2 heavy- (H) chain V region amino acid substitutions. Because both variant antibodies contained substitutions at H chain position 35 (H35), and because this is a site of recurrent mutation in 26-10 hybridoma variants demonstrating reduced antibody affinity for digoxin (D.J. Panka, S.Y. Shaw, D.R. Parks, & M.N. Margolies, unpubl. obs.), we undertook mutagenesis experiments to define the contribution of this position to 26-10 antibody specificity. First, we established that the position 35 mutations observed in the variants were responsible for the reduced affinity of the variants. To examine the influence of other position 35 substitutions on hapten binding, additional mutants were generated. The 26-10 antibody proved sensitive to position 35 substitutions, with most mutant antibodies displaying not only reduced affinity for digoxin, but also altered fine specificity. Subsequently, the X-ray crystal structure of 26-10 Fab in complex with digoxin was determined (Kinemage 1; Jeffrey et al., 1993) and showed that the H35 Asn not only provides hapten contacts but is also involved in a hydrogen bond network with 2 other contact residues. The structure enabled us to model the mutant antibodies and correlate the models with the results of the binding studies.

The results of the modeling and binding studies indicate that the H35 Asn is an important contact residue and structural element of antibody 26-10, and the identity of the amino acid at this position can greatly affect hapten recognition. In addition, the effect of H35 amino acid substitutions upon specificity in other antibodies suggests that the residue at this position may be important for maintenance of binding site architecture and function for many antibodies.

Results

The 26-10 hybridoma variants L1B1 and R3 were selected by fluorescence-activated cell sorting (FACS) due to their reduced staining by a conjugate of digoxin, human serum albumin (HSA), and phycoerythrin. Antibodies produced by these hybridoma variants had no detectable binding in a saturation equilibrium assay (data not shown). Using a solid-phase assay that is more sensitive to low-affinity binding, both L1B1 and R3 demonstrated some binding above background to a conjugate of digoxin and HSA (Table 1). The binding of L1B1 and R3, however, was much lower than that of a similar concentration of 26-10 antibody (Table 1) and was consistent with affinities lower than can be measured using the saturation equilibrium assay (see below).

Table 1. *Digoxin binding of 26-10 variant antibodies*[a]

Antibody/mutant	CPM bound
26-10	9,705 ± 750
R3[b]	1,050 ± 55
L1B1[c]	538 ± 22
No antibody	215 ± 10

[a] Antibody solutions of similar concentrations were incubated in wells of plates coated with a conjugate of digoxin and human serum albumin, the plates washed, and antibody detected by radioiodinated goat anti-mouse-Fab.

[b] Contains Lys for Asn substitution at H35.

[c] Contains Tyr for Asn substitution at H35 and Met for Arg substitution at H38.

The H chain of secreted L1B1 antibody appeared more acidic, and that of R3 appeared more basic, than the H chain of secreted 26-10 antibody when analyzed by 2-dimensional SDS-PAGE (data not shown). In addition, the H chain of R3 cell surface antibody appears to be of slightly lower molecular weight than that of 26-10, although the cell surface R3 antibody H chain is larger than the secreted 26-10 and R3 H chains (data not shown). The R3 and L1B1 light (L) chains were indistinguishable from that of 26-10 (data not shown).

Sequence analysis of variant antibodies

Amino acid and nucleotide sequencing of R3 and L1B1 antibody V regions were undertaken to determine the basis for the altered hapten binding. Automated Edman degradation of the R3 H chain extended for 58 cycles, with the use of *o*-phthalaldehyde (OPA) treatment at cycle 14 (at which Pro is N-terminal). The sequence was identical to that of 26-10 except for substitution of Lys for Asn at cycle 35 (Fig. 1). This substitution was confirmed by the sequence of the CNBr peptide N-terminal at position 35 (Lys), which extended through position 76 (Kabat numbering; Kabat et al., 1991). This sequence was otherwise identical to 26-10. The CNBr peptide N-terminal at position 101 was also sequenced into C_{H1} and showed no differences from 26-10. The N-terminal sequence of the intact R3 L chain (55 cycles, aided by extended cleavage of the phenylthiocarbamyl at cycle 8 and OPA treatment at cycles 12 and 49) revealed no differences from that of 26-10 (not shown).

Residues 1–61, 81–98, and 101–113 of the L1B1 H chain were also identified by amino acid sequencing. Two substitutions relative to 26-10 were found: replacement of Asn with Tyr at H chain position 35 and Arg with Met at H chain position 38 (H 38). The partial amino acid sequence of L1B1 L chain V region (positions 1–37 and 55–108) was identical to 26-10.

Complete nucleotide sequencing of cloned, PCR-amplified H and L V region cDNA of R3 and L1B1 confirmed and extended these results and those of cDNA sequencing by chemical cleavage (see Materials and methods). No additional differences between 26-10 and the variant antibody V regions were found.

Mutagenesis analysis of variants

Mutagenesis experiments were first undertaken to determine the individual contributions of the 2 amino acid substitutions in the L1B1 H chain to the binding defect. Mutant antibodies with ei-

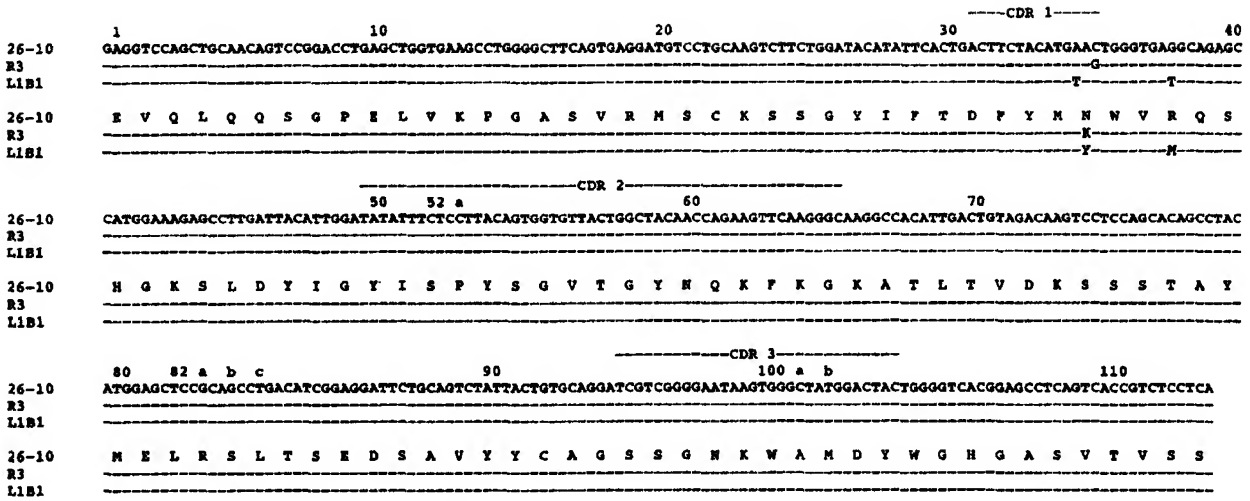

Fig. 1. Nucleotide and amino acid sequences of 26-10, R3, and L1B1 H chains. Amino acid sequences were translated from nucleotide sequences and confirmed in part by protein sequence analysis. Amino acid sequences are given in 1-letter code. Amino acid residue numbering and complementarity determining regions are as defined by Kabat et al. (1991). A dash indicates identity to the topmost sequence. Complete genomic and cDNA nucleotide and partial protein sequences of 26-10 V regions were reported (Novotny & Margolies, 1983; Mudgett-Hunter et al., 1985; Hudson et al., 1987; Near et al., 1990; Schildbach et al., 1991).

ther the H35 Tyr for Asn (H:Asn-35-Tyr) or H 38 Met for Arg (H:Arg-38-Met) substitution were constructed. In addition, antibody H:Asn-35-Lys was engineered to confirm the results for the spontaneous variant R3. The mutagenic oligonucleotides used are listed in Table 2. Both the H:Asn-35-Tyr and H:Asn-35-Lys antibodies demonstrate greatly reduced binding to digoxin–HSA relative to 26-10wt (Table 3). Antibody 26-10wt ($K_a = 9.1 \times 10^9\ M^{-1}$; see below) is the product of expression of the unmutated 26-10 H chain in 26-10κ cells and differs from 26-10 in H chain isotype (γ2a for 26-10 and γ2b for 26-10 wt), but not in hapten recognition (data not shown). Antibodies H:Asn-35-Tyr and H:Asn-35-Lys also have lower binding than the engineered 26-10 mutant H:Tyr-50-Asp, which was used as a control because it has an affinity near the lower limit of measurement of the saturation equilibrium assay ($2.3 \times 10^6\ M^{-1}$; Schildbach et al., 1993a). The low binding of antibodies H:Asn-35-Tyr and H:Asn-35-Lys in the solid-phase assay is therefore consistent with their lack of detectable binding in the saturation equilibrium assay. These results also confirm the observation made of the spontaneous variants: nonconservative substitutions at H35 can greatly reduce (>10^4-fold) the affinity for digoxin of 26-10 mutant antibodies.

Table 2. *Mutagenic oligonucleotides*

	Sequence
Mutant	5′ 3′
H:Asn-35-Tyr	CT CAC CCA GTA CAT ATA GAA G
H:Asn-35-Lys	CT CTG CCT GAC CCA TTT CAT GTA GAA G
H:Asn-35-Ala	CT CAC CCA GGC CAT GTA GAA GTC
H:Asn-35-Asp	GCT TTG CCT CAC CCA GTC CAT GTA GAA GTC
H:Asn-35-Val	CT CAC CCA GAC CAT GTA GAA GTC
H:Asn-35-Gln	CT CAC CCA CTG CAT GTA GAA GTC
H:Asn-35-Leu	CT CAC CCA GAG CAT GTA GAA GTC
H:Asn-35-Thr	CT CTG CCT GAC CCA GGT CAT GTA GAA G
H:Arg-38-Met	CC ATG ACT CTG CAT CAC CCA GTT C

[a] Oligonucleotides are anti-sense and complementary, annealing from H chain position 31 to 38 or 40 for H35 mutants, and from position 34 to 42 for H:Arg-38-Met (see Fig. 2). Nucleotides differing from wild type are underlined. Oligonucleotides for H:Asn-35-Asp, H:Asn-35-Lys, and H:Asn-35-Thr also contain silent mutations to increase differences in melting temperatures of mutant oligonucleotides annealed to mutated and unmutated 26-10 H chain sequence during dot blot hybridization screening (Sambrook et al., 1989).

Table 3. *Digoxin binding of engineered 26-10 mutant antibodies*[a]

Antibody/mutant	CPM bound[b]
26-10wt	13,608 ± 82
H:Asn-35-Lys	2,562 ± 72
H:Asn-35-Tyr	445 ± 5
H:Tyr-50-Asp[c]	8,622 ± 112
No antibody	215 ± 10

[a] Antibody solutions of similar concentrations were incubated in wells of plates coated with a conjugate of digoxin and human serum albumin, the plates washed, and antibody detected by radioiodinated goat anti-mouse-Fab.

[b] Discrepancies between CPM listed here and in Table 1 are due in part to different recognition by the radioiodinated goat anti-mouse-Fab of 26-10 and the spontaneous variants (heavy chain isotype γ2a) versus 26-10wt and the engineered mutants (heavy chain isotype γ2b).

[c] The engineered 26-10 mutant H:Tyr-50-Asp is included as a control because its affinity for digoxin (2.3×10^6 M^{-1}) approaches the lower limit of measurement by the solution-phase affinity assay (Schildbach et al., 1993a).

Affinity measurements established that H:Arg-38-Met and 26-10wt have equivalent affinities for digoxin (data not shown). The greatly reduced affinity for digoxin of L1B1 is therefore solely due to the H35 Tyr for Asn substitution.

Mutagenesis analysis of H35

It was reasoned that more conservative substitutions than Tyr (L1B1) or Lys (R3) for Asn may have less drastic effects and would provide additional insight into the role of H:Asn-35 in the hapten binding of 26-10. Therefore, a panel of 26-10 antibodies mutated at H35 was constructed. In antigen combining sites, Asn residues often form hydrogen bonds through their side-chain atoms to other side chains or to the main chain (Padlan, 1990). Therefore Gln, Asp, and Thr, which are capable of forming hydrogen bonds, and sterically similar amino acids incapable of forming hydrogen bonds (Leu for comparison to Asn, Val for comparison to Thr, and Ala) were substituted for Asn. The mutant antibodies and the mutagenic oligonucleotides used in their creation are listed in Table 2.

The affinities of the mutant antibodies for digoxin are compared to that of 26-10wt in Table 4. Replacing Asn with Gln (H:Asn-35-Gln) causes an approximately 10-fold drop in affinity, whereas replacement with Val (H:Asn-35-Val) reduces affinity approximately 90-fold. Substituting Thr, Leu, or Ala for the H35 Asn (H:Asn-35-Thr, H:Asn-35-Leu, and H:Asn-35-Ala, respectively) reduces affinity for digoxin approximately 200-fold, whereas replacement with Asp (H:Asn-35-Asp) reduces affinity 1,400-fold.

The relative affinities of the antibodies for digoxin analogues were measured using a competition assay (Tables 5, 6). A summary of the analogue structures is given in Table 5, by reference to Figure 2. Analogues chosen included those demonstrating altered binding to the mutant H:Asn-35-Ala in preliminary assays. The values are reported in Table 6 as relative K_i, which is the K_d of an antibody for an analogue as determined by a competition assay, normalized to the K_i of digoxin for that antibody.

Table 4. *Affinity of H35 mutants for digoxin*[a]

Antibody	Affinity ($\times 10^{-5}$ M^{-1})
26-10wt	91,000 ± 10,000
H:Asn-35-Gln	8,400 ± 1,000
H:Asn-35-Val	970 ± 120
H:Asn-35-Thr	440 ± 70
H:Asn-35-Leu	390 ± 50
H:Asn-35-Ala	380 ± 60
H:Asn-35-Asp	66 ± 16
H:Asn-35-Lys	<10[b]
H:Asn-35-Tyr	<10[b]

[a] Affinities for digoxin were measured in a saturation equilibrium assay using filtration through glass fiber filters to separate bound from free tritiated ligand (see Materials and methods).

[b] Affinity below lower limit of this assay (10^6 M^{-1}).

The K_i values for digoxin agreed well with the K_d determined by the saturation equilibrium assay (data not shown).

As described previously for 26-10 (Schildbach et al., 1991), the 26-10wt antibody has lowered affinity for digoxin analogues with 16-position substitutions (see Fig. 2; Tables 5, 6). The affinity decreases as the size of the 16-position substituent increases. Gitoxin, which has a 16-hydroxyl (16-OH) group, is bound by the 26-10wt antibody with 6-fold lower affinity than digoxin. Gitaloxin, with a 16-formyl group, is bound with 32-fold lower affinity. The analogues 16-acetylgitoxin, oleandrin, and oleandrigenin all have 16-acetyl groups and are bound with even lower affinities (250–9,900-fold reductions). The affinities for these 3 congeners, however, are affected by the identity of the substituent at the 3-position: 16-acetylgitoxin, with a 3-tridigitoxose, is bound with the highest affinity of the 3, whereas oleandrin, with a 3-oleandrose, and oleandrigenin, with a 3-OH, are bound with progressively lower affinities. Dihydrodigoxin, which has a saturated C20–C22 lactone bond, is bound by antibody 26-10wt with 1,300-fold lower affinity than digoxin.

Antibody H:Asn-35-Gln exhibits a specificity similar to 26-10wt (Table 6). The only possible difference is in recognition of oleandrigenin, which H:Asn-35-Gln binds with an affinity below the limits of this assay, precluding direct comparison to 26-10wt.

Table 5. *Structure of digoxin and digoxin analogues*

	Substituents at positions[a]			
Analogue	3	12	16	C20–C22 bond
Digoxin	Tridigitoxose	-OH		Unsaturated
Gitoxin	Tridigitoxose		-OH	Unsaturated
Gitaloxin	Tridigitoxose		-CHO	Unsaturated
16-Acetylgitoxin	Tridigitoxose		$-COCH_3$	Unsaturated
Oleandrin	Oleandrose		$-COCH_3$	Unsaturated
Oleandrigenin	-OH		$-COCH_3$	Unsaturated
Dihydrodigoxin	Tridigitoxose	-OH		Saturated

[a] Cardenolide numbering scheme is shown in Figure 2.

Table 6. *Relative K_i values of N35 mutants for digoxin analogues*[a]

Analogue	26-10wt	H:Asn-35-Gln	H:Asn-35-Val	H:Asn-35-Thr	H:Asn-35-Leu	H:Asn-35-Ala	H:Asn-35-Asp
Digoxin	1	1	1	1	1	1	1
Gitoxin	6	11	11	4	13	14	0.9
Gitaloxin	32	51	29	17	41	3	6
16-Acetylgitoxin	250	180	63	68	86	8	49
Oleandrin	920	740	220	>180	260	19	>47
Oleandrigenin	9,900	>7,100	>760	>180	>460	14	>47
Dihydrodigoxin	1,300	2,700	110	94	190	190	>47

[a] K_i of antibodies for digoxin analogues were determined in a solution-phase competition assay (see Materials and methods). K_i is K_d as determined by competition assay. Values were normalized to the K_i for digoxin for each antibody. Values for those haptens that at the highest concentrations used in the assay (10 μM) inhibited less than 50% of binding of [^{3}H]digoxin are denoted as greater than the highest measurable relative K_i.

Antibodies H:Asn-35-Val, H:Asn-35-Thr, and H:Asn-35-Leu all have similar fine specificities, demonstrating relative affinities 3–4-fold higher for 16-acetylated haptens and 7–14-fold higher for dihydrodigoxin compared to 26-10wt. The only difference between the 3 mutants is that H:Asn-35-Thr has a 3-fold higher relative affinity for gitoxin than the others. As is the case for H:Asn-35-Gln, these mutant antibodies bind some of the 16-acetylated compounds with affinities too low to be measured.

Antibody H:Asn-35-Ala also demonstrates a higher relative affinity for dihydrodigoxin than does 26-10wt. More significantly, the relative affinities of H:Asn-35-Ala for gitaloxin and the 16-acetylated haptens were dramatically increased: all are bound with affinities approximately equal to or significantly higher than for gitoxin. The affinity of H:Asn-35-Ala for oleandrigenin (K_i = 360 nM) is actually greater than that of 26-10wt (K_i = 720 nM). Antibody H:Asn-35-Asp also possesses a unique specificity: this mutant binds gitoxin and digoxin equally, and binds gitaloxin and 16-acetyldigoxin with improved relative affinities, compared to 26-10wt. The low affinity of H:Asn-35-Asp precluded measurement of the K_i for oleandrin, oleandrigenin, and dihydrodigoxin.

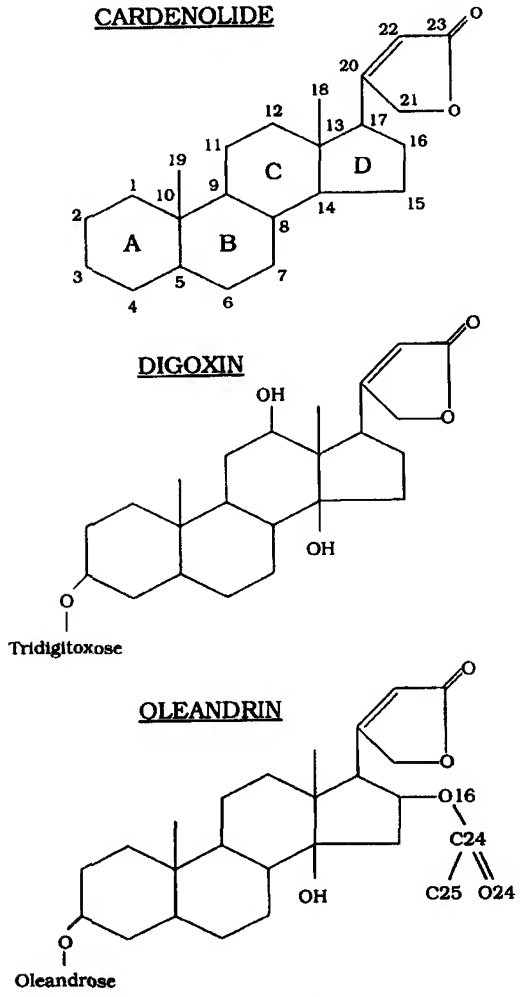

Fig. 2. Diagrams of the cardenolide numbering system, digoxin (digoxigenin tridigitoxose), and oleandrin including the numbering for the 16-acetyl moiety (from Kartha & Go, 1981).

Molecular modeling analysis

The X-ray crystal structure of the 26-10 Fab complexed with digoxin was determined subsequent to completion of the mutagenesis experiments (Kinemage 1; Jeffrey et al., 1993). The structure shows that the H:Asn-35 contacts (as defined by Sheriff et al., 1987a) the D ring (atoms C16 and C17) and the lactone (atoms C20, C21, and C22) of digoxin (P.D. Jeffrey, unpubl. obs.; Figs. 2, 3; Kinemages 1, 2). In addition, H:Asn-35 forms hydrogen bonds with the hydroxyls of H:Tyr-47 and H:Ser-95, both of which are hapten contact residues. The electron density maps were interpreted as the H:Asn-35 $N_{\delta 2}$ serving as a hydrogen bond donor to the H:Tyr-47 O_η and the H:Ser-95 O_γ acting as a hydrogen bond donor to the H:Asn-35 $O_{\delta 1}$. The electron density maps, however, are consistent with an H:Asn-35 orientation in which the $O_{\delta 1}$ and $N_{\delta 2}$ are rotated 180° about the C_β–C_γ bond and the pattern of hydrogen bond donors and acceptors is altered.

We used the 26-10 Fab:digoxin structure as the basis for modeling the mutants. A description of the modeling procedure, including assumptions made and the resulting limitations of the method, is given below (see Materials and methods). As a control for the modeling procedure, an H:Asn-35 side chain was modeled into the 26-10 structure. The 2 lowest-energy modeled side-chain conformations included a conformation similar to that of the crystal structure (second lowest; Fig. 4) and a conformation rotated approximately 180° about the C_β–C_γ bond

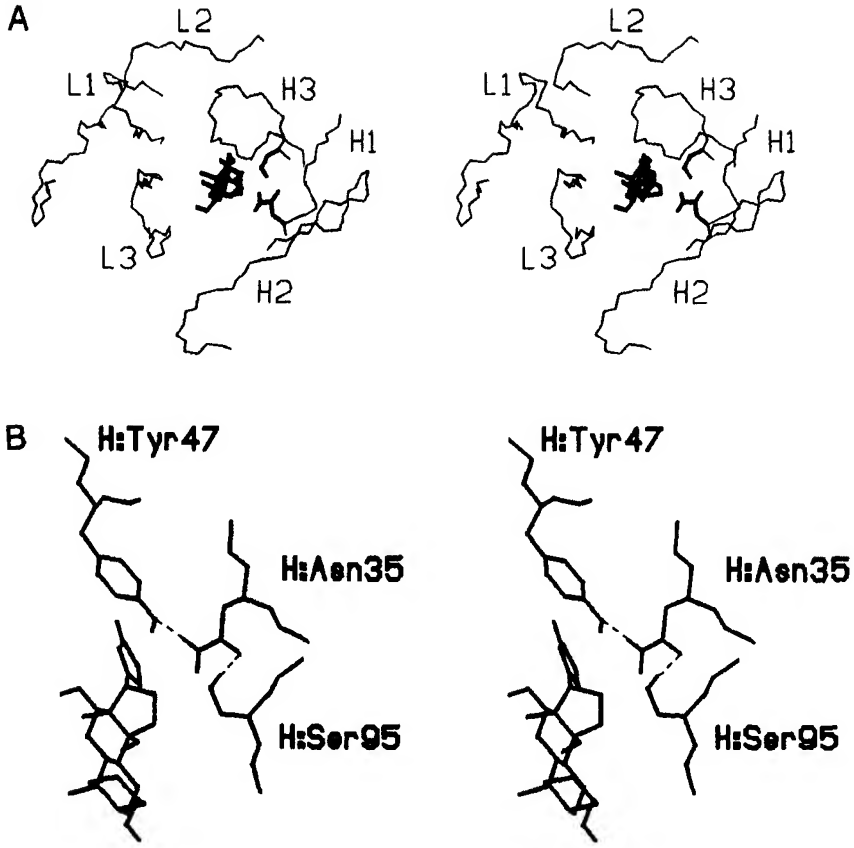

Fig. 3. **A:** Stereo view of 26-10 CDRs and bound digoxigenin from the 26-10 Fab:digoxin crystal structure (Jeffrey et al., 1993). View is from solvent into the binding site. Depicted in bold lines (center of diagram) are digoxigenin and residues H:Asn-35 (in first H chain CDR, H1) and H:Ser-95 (in H3). Hydrogens are shown explicitly only on potential hydrogen bond donors. **B:** Stereo view showing detail of bound digoxigenin, H:Asn-35, H:Tyr-47 (from framework region 2), and H:Ser-95. View is rotated 130° about the horizontal axis from view shown in top panel. Amino acids are shown with the main chain through the C_α atoms of the adjacent residues. Hydrogens are shown explicitly only on potential hydrogen bond donors. Hydrogen bonds are shown as dashed lines.

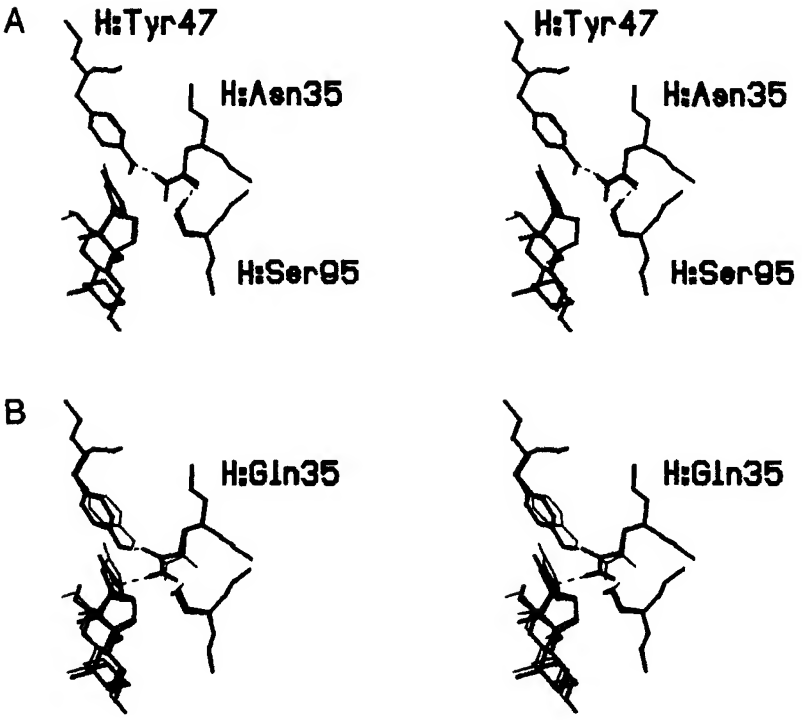

Fig. 4. Stereo views of modeled H35 mutants complexed with digoxigenin. **A:** H:Asn-35-Asn (modeled 26-10). **B:** H:Asn-35-Gln. The H35 residue is shown with digoxigenin, H:Tyr-47, and H:Ser-95 (bold lines). The models are superimposed upon the 26-10 structure (thin lines) for comparison. Amino acids are shown with main-chain atoms through the C_α of adjacent residues. Hydrogens are shown explicitly only on potential hydrogen bond donors. Hydrogen bonds are shown as dashed lines.

(not shown). Both of these modeled conformations represent possible orientations for the side chain (see above) and are consistent with the 26-10:digoxin crystal structure.

Noting that the H:Asn-35-Gln mutant antibody retained the wild-type specificity and that Gln, like Asn, may be able to participate in a hydrogen bond network, we modeled the H:Asn-35-Gln mutant to ascertain whether the substituted Gln could maintain the network (Fig. 4). The lowest-energy conformation for the Gln side chain allows formation of a hydrogen bond between H35 and the H:Tyr-47 hydroxyl but does not permit formation of a hydrogen bond with H:Ser-95 without reorientation of the H:Ser-95 side chain. Although the Gln side-chain $N_{\epsilon 2}$ protrudes slightly into the binding site, causing energetically unfavorable contacts with the digoxigenin lactone when the hapten is inserted into the binding site, these van der Waals energies were significantly reduced during an energy minimization step through minor positional shifts by the Gln side chain. This result suggests that these unfavorable contacts may account for the 10-fold lower affinity of H:Asn-35-Gln for digoxin relative to 26-10wt. A hydrogen bond is possible between the Gln amide and the O21 of the digoxin lactone.

Several other mutants were also modeled. The only other mutant that maintained the hydrogen bonds seen in 26-10 was H:Asn-35-Asp (not shown), although the polarity of the hydrogen bond between H35 and H:Tyr-47 was reversed. Although this antibody demonstrates significantly altered hapten binding relative to wild type (Tables 4, 6), the negative charge of Asp rather than a structural effect due to the H35 substitution may be responsible. Modeling experiments suggest that none of the mutants with uncharged H35 residues, with the exception of Gln, are able to reproduce the hydrogen bonding seen in 26-10 and correspondingly do not show wild-type specificity.

To seek explanations for the altered fine specificity of the Ala mutant, hapten docking experiments for both 26-10 and H:Asn-35-Ala were conducted (see Materials and methods). The models of 26-10 and H:Asn-35-Ala each docked with oleandrin differ (Fig. 5). The low-energy position of the oleandrin 16-acetyl group in the H:Asn-35-Ala model is forbidden in the 26-10 model because of unfavorable contacts with the 26-10 H:Asn-35. In addition, the position of the H:Tyr-33 side chain in the 26-10:oleandrin model is shifted relative to the position of the side chain in the 26-10:digoxin crystal structure. The position of H:Tyr-33 does not differ between the models of H:Asn-35-Ala complexed with digoxigenin or with oleandrin.

Results of docking dihydrodigoxigenin into the binding sites of 26-10 and H:Asn-35-Ala are shown in Figure 6 (thick lines),

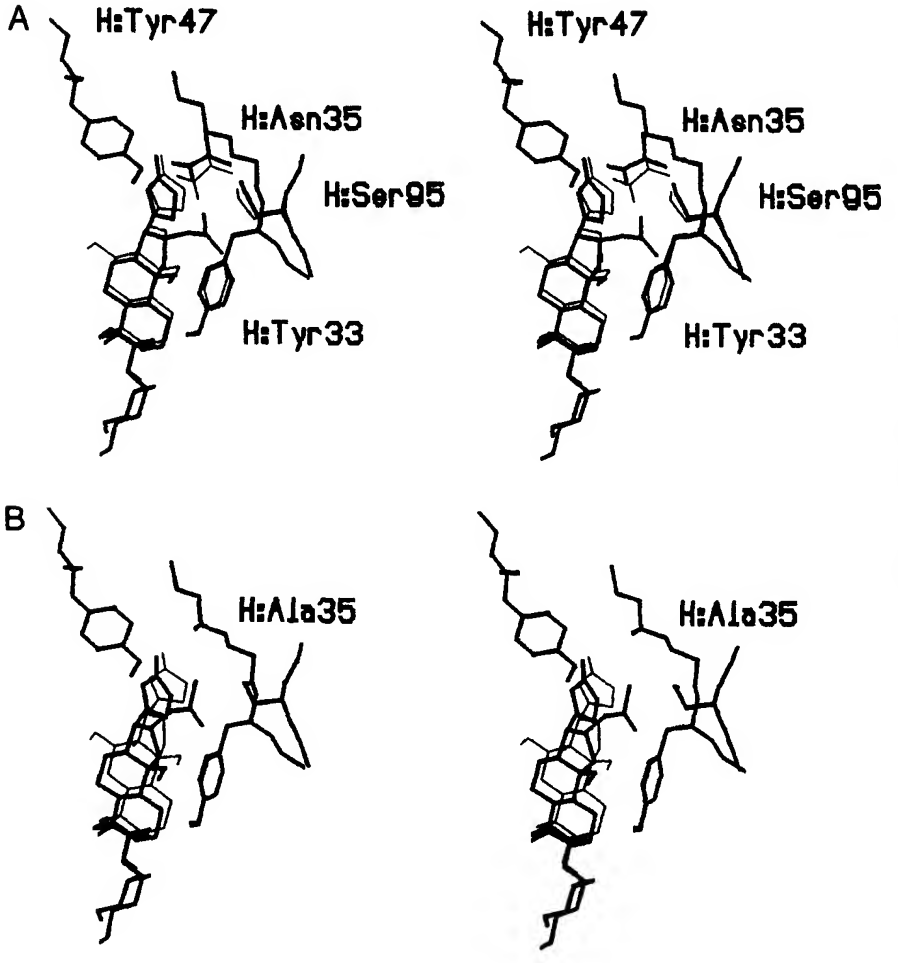

Fig. 5. Stereo views of modeled complexes of (**A**) 26-10 and (**B**) H:Asn-35-Ala with oleandrin. Oleandrin, H:Tyr-33, H:Tyr-47, H:Ser-95, and the H35 residue are shown (thick lines) with the corresponding side chains and hapten molecules from modeled complexes of the antibodies with digoxigenin (thin lines). The main-chain atoms of amino acids are displayed through the C_α of adjacent residues. Hydrogens are shown explicitly only on potential hydrogen bond donors.

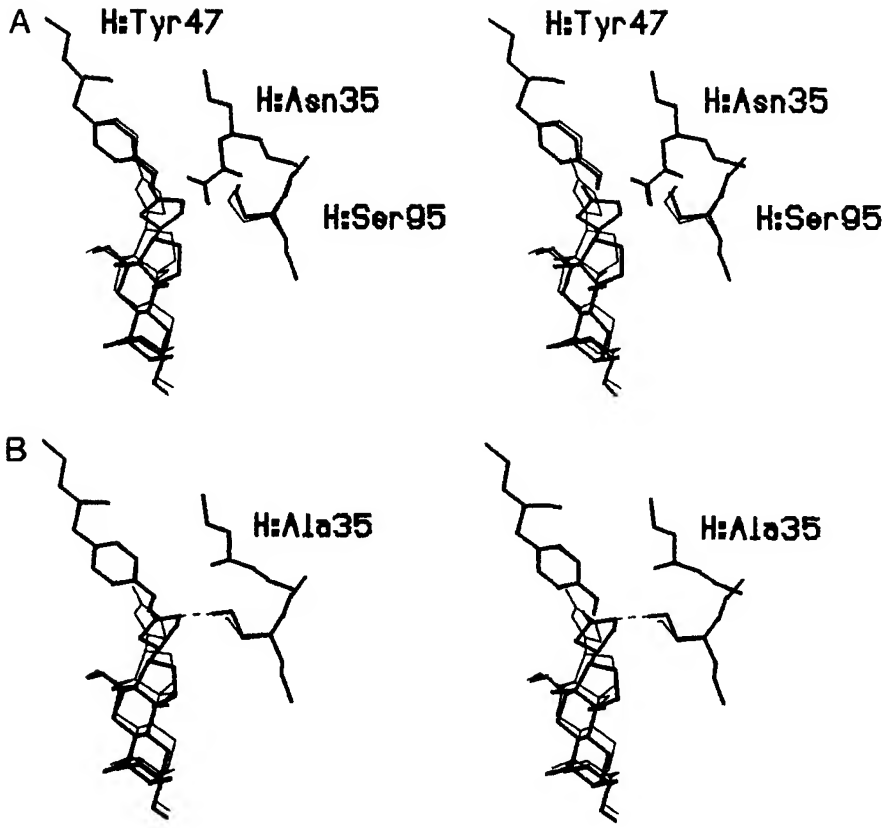

Fig. 6. Stereo views of modeled complexes of **(A)** 26-10 and **(B)** H:Asn-35-Ala with dihydrodigoxigenin (bold lines). Models are superimposed upon those of complexes of their respective antibodies with digoxigenin (thin lines). The main-chain atoms of amino acids shown through the C_α of adjacent residues. Hydrogens are shown explicitly only on potential hydrogen bond donors. Hydrogen bonds are shown as dashed lines.

compared to digoxigenin docked into the same binding sites (thin lines). The saturated lactone of dihydrodigoxigenin, unlike that of digoxigenin, is not planar, disrupting the complementarity between antibody and hapten. In both 26-10 and H:Asn-35-Ala, the entire dihydrodigoxigenin molecule, and the lactone in particular, is shifted relative to the position of digoxin bound in the same site. Despite the shift, unfavorable contacts remain between the 26-10 H:Asn-35 side chain and the lactone. Substitution of Ala for Asn avoids these unfavorable contacts. In addition, the lactone of dihydrodigoxigenin bound by H:Asn-35-Ala is rotated approximately 30° about the C17–C20 bond, relative to the lactone of dihydrodigoxigenin docked into the 26-10 binding site. This conformation is lower in energy than the configuration in the 26-10 model and also allows a hydrogen bond to be formed between the hydroxyl of H:Ser-95 and the O21 of dihydrodigoxigenin.

The modeled hapten:antibody complexes therefore suggest that haptens dihydrodigoxigenin and oleandrigenin can adopt lower energy conformations within the binding site of H:Asn-35-Ala that are disallowed in the 26-10 binding site.

Discussion

The high affinity of antibody 26-10 for digoxin is derived largely from shape complementarity and the attendant desolvation of the complementary surfaces; there are no apparent energetic contributions from ionic or hydrogen bonding interactions (Jeffrey et al., 1993). Consistent with this observation, we previously reported that mutations of a noncontact residue can significantly reduce affinity for digoxin, presumably by altering the shape of the binding cavity (Schildbach et al., 1993b).

The binding of many of the 26-10 H35 variant and mutant antibodies described here can also be attributed to the effects of amino acid substitutions on the shape of the binding site. Spontaneous variant antibodies L1B1 and R3, and the engineered mutant antibodies containing their H35 substitutions (H:Asn-35-Tyr and H:Asn-35-Lys, respectively) have greatly reduced affinity for digoxin, due to the introduction of bulky side chains into a region known to be of tight complementarity (Fig. 3; Kinemage 2). The lowered affinities for digoxin of the Val, Leu, Thr, or Ala mutants appear too large to be accounted for by the reduction in contact area alone. Although the H:Asn-35 side chain is buried in the antibody:hapten complex, the side chain has only a 7-Å^2 solvent-exposed surface when uncomplexed (measured using a 1.5-Å diameter probe; Lee & Richards, 1971). The approximately 3 kcal loss in binding energy (where binding energy is calculated by $\Delta G = RT \ln K_d$ and R is the gas constant, T is 293 K, and K_d is the experimentally determined dissociation constant of the antibodies for digoxin) of the Val, Leu, Thr, and Ala mutants, relative to 26-10wt, is far greater than expected according to standard estimates (25–47 cal/Å^2 of surface area of complex; Chothia, 1974; Eisenberg et al., 1989; Sharp et al., 1991). Destabilization of the antibody:hapten complex by an unoccupied volume at the interface, analogous to the reduced stability caused by substitution of small for large amino acids within a protein core (Eriksson et al., 1992), is also an un-

satisfactory explanation for the reduced affinities because H:Asn-35-Leu has a 200-fold lower affinity for digoxin than 26-10wt, despite similar volumes of Leu and Asn. Given the similar affinities for digoxin conferred by dissimilar H35 substitutions (Val, Thr, Leu, Ala), the altered hapten binding of these antibodies may be due largely to loss of the hydrogen bonds formed by the wild-type Asn.

The hydrogen bonds formed by H:Asn-35 may contribute to the binding of 26-10 by stabilizing the side-chain conformations of the contact residues H:Asn-35, H:Tyr-47, and H:Ser-95, reducing the entropic penalty incurred when the mobility of the side chains is limited during complexation with hapten. In addition, the hydrogen bonds may orient the side chains of these residues in positions that optimize the area of contact between antibody and hapten.

Molecular modeling studies of antibodies with substitutions at position H35 suggest that Gln and Asp can maintain one or both of these hydrogen bonds (Fig. 4). The model of H:Asn-35-Gln suggests that the moderately reduced affinity of this antibody is due to unfavorable contacts between hapten and the Gln side chain. A hydrogen bond between the Gln and the O21 of digoxin may partially compensate for these unfavorable contacts. The altered hapten binding of antibody H:Asn-35-Asp, however, is probably due to introduction of the Asp negative charge, which makes desolvating the binding site of the Asp mutant energetically costly, relative to desolvating the 26-10wt binding site. The similarities in the fine specificity of antibodies 26-10wt and H:Asn-35-Gln are consistent with similar binding site structures of these antibodies. These results, taken together with the binding of the other mutant antibodies with neutral H35 substitutions, support the contention that the hydrogen bonding of H:Asn-35 is essential to maintain the local binding site structure and the specificity of the antibody.

Although the altered affinity of the Ala mutant may be the result of the effect of this substitution on other residues (e.g., H:Tyr-47 and H:Ser-95) through hydrogen bond loss, the altered fine specificity appears to be due to the smaller size of Ala compared to Asn. Docking experiments (Figs. 5, 6) suggest that H35 Ala allows more space at the hapten:antibody interface than does H35 Asn, permitting dihydrodigoxigenin and oleandrigenin to adopt low energy conformations within the binding site of H:Asn-35-Ala that are disallowed in the 26-10 binding site. In contrast, the altered fine specificity of H:Asn-35-Asp may be due to the introduction of the negatively charged side chain, which interacts more favorably than the neutral Asn side chain with the 16-hydroxyl of gitoxin. In principle, this model may be tested by pH titration of the negative charge of the Asp side chain in the affinity or specificity assays. Presumably effects due to the charge of Asp would diminish as the side chain is protonated. Under the acidic conditions required to protonate Asp (pH ~3.5), however, the apparent affinity of all antibodies tested was considerably reduced. In particular, mutant antibodies H:Asn-35-Asp and H:Asn-35-Leu had no detectable specific binding of digoxin under these conditions, preventing characterization of their binding as a function of pH.

Not all contact residues in 26-10 are as sensitive to replacement as is H:Asn-35. We previously described mutations of the CDR2 contact residue H:50-Tyr (Fig. 1) that reduce affinity and alter fine specificity due to a reduction in the size of the hapten:antibody interface (Schildbach et al., 1993a). Many of the 26-10 H35 mutant antibodies described here also display reduced affinity and altered fine specificity resulting from substitution of a hapten contact residue. However, mutations at H35 and at H50 exhibit different patterns of constraints on hapten recognition. For example, substitutions larger than Asn at H35 reduced affinity significantly (10-fold for Gln or greater than 4,000-fold for Lys or Tyr), whereas replacement of H50 Tyr with Trp had little effect (Schildbach et al., 1993a). Replacement of H:Asn-35 with smaller residues (Val, Thr, Leu, Ala) resulted in similar reductions in affinity for digoxin (100–200-fold), but substitution of H:Tyr-50 with Asn, His, Leu, Ala, or Gly resulted in a greater range of affinities (reductions of 30–3,000-fold). Furthermore, the difference in affinities for digoxin of antibodies with H35 Asn vs. H35 Asp is 1,400-fold, whereas the difference for antibodies with these residues at H50 is 130-fold.

These differences in the results of mutagenesis of 2 different contact residues reflect in part their different locations in the binding site. Position H50 is near the mouth of the binding site, whereas H35 is located deep within the binding pocket (Jeffrey et al., 1993). The relative solvent accessibility of H50 compared to H35 in the 26-10:digoxin complex may account for the less detrimental effect of the negative charge of Asp on binding when located at H50 than when at H35. In addition, the location of H35 deep within the antibody:hapten complex places stricter restraints on the size of residues at H35 than on those at H50. The different roles of these side chains in recognition is also responsible for the differences in the effects of mutation. Although H:Tyr-50 contributes far more hapten contact area than does the H:Asn-35 (33 vs. 7 $Å^2$; calculated using a 1.5-Å diameter probe [Lee & Richards, 1971]), the H:Asn-35 contributes to the structure of the binding site via hydrogen bonds to H:Tyr-47 and H:Ser-95, both of which are contact residues. The H:Tyr-50 side chain does not form hydrogen bonds with hapten or with other antibody residues.

The importance of the identity of the H35 residue to hapten recognition has been demonstrated for other antibodies. Substitution of Asp for Asn at H35 of the anti-*p*-azophenylarsonate antibody 36-71 caused a 70-fold decrease in affinity, and substitution of Gln reduced affinity greater than 350-fold (Sompuram & Sharon, 1993). Substitution of Ala, Gln, or Asp for Asn at H35 for the corresponding germline antibody 36-65 caused virtual loss of binding of arsonate (Parhami-Seren et al., 1993). Substitution of Ala at H35 of antibodies 36-65 and 36-71 resulted however in greatly increased affinity for sulfonate (Kussie et al., 1994). As for 26-10, the H:Asn-35 of 36-71 not only contacts hapten in the modeled complex (Strong et al., 1991) but forms hydrogen bonds with contact residues H47 (Trp) and H95 (Ser). In the phosphorylcholine-binding myeloma protein McPC603, H:Glu-35 forms a hydrogen bond with the hydroxyl of the contact residue L:Tyr94. Mutagenesis of H:Glu-35 to Gln in the McPC603 Fv (Glockshuber et al., 1991), or to Ala in the related S107 anti-phosphorylcholine antibody (Rudikoff et al., 1982; Diamond & Scharff, 1984), greatly reduces the affinity for phosphorylcholine. The Ala substitution also confers a different specificity upon the S107 antibody, causing it to recognize double-stranded DNA (Rudikoff et al., 1982). The lost affinity for phosphorylcholine in the McPC603 mutant may be the result of either the lost negative charge of Glu, or the structural effects caused by alteration of the hydrogen bonding of H:Glu-35 (Glockshuber et al., 1991). For the mutants of 36-65 and 36-71, either a lost hydrogen bond between hapten and antibody or more indirect structural effects may have caused the reduced

affinity for hapten. Regardless of the exact cause, however, H35 substitutions in these antibodies and in 26-10 can significantly alter antibody binding.

Although the identity of the residue at H35 is central to the specificity exhibited by 26-10, McPC603, 36-65, and 36-71, there is limited homology among them. The antibodies differ in V region sequence (Kabat et al., 1991) and in the effect of mutation at sites other than H35 (Glockshuber et al., 1991; Parhami-Seren et al., 1993; Sompuram & Sharon, 1993). The same amino acid substitution in these antibodies at a site other than H35 can have substantially different effects on binding function, indicating differences between these antibodies in the modes or mechanisms of hapten binding. Substitutions at H35 in all of these antibodies, however, can alter affinity and specificity. The importance of H35 to binding function in these antibodies probably reflects a shared structural role of the H35 residue. The structure of H chain CDR1 is relatively conserved among antibodies (Chothia et al., 1989); this structure may position H35 in a crucial site at the bottom of the binding site.

Examination of the sequences of antibody V regions (Kabat et al., 1991) shows that Asn occurs frequently at murine H chain position 35 as does His, Glu, and Ser. Each of these residues is capable of forming hydrogen bonds, and therefore H35 may often be involved in maintaining the local structure of the antibody binding site. Certainly, substitutions at this site can profoundly affect antibody function. This position, therefore, is an obvious focus of antibody engineering designed to alter specificity or introduce a new specificity.

Materials and methods

Cell lines

The derivation of the murine anti-digoxin hybridoma 26-10 (IgG2a, κ) was described (Mudgett-Hunter et al., 1982). The isolation of the 26-10 hybridoma subclone 26-10P2 and the procedure used for cloning the spontaneous hybridoma variants 26-10P2.6R3 (referred to herein as R3) and 26-10P2.28L1B1 (referred to herein as L1B1) by 3 cycles of 2-color FACS from the 26-10 hybridoma subclone P2 were described (Schildbach et al., 1991). Cell line 26-10κ, a spontaneous H chain loss variant of 26-10, was subcloned and selected on the basis of H chain isotype loss as determined by screening supernatants using an isotype ELISA. Cell line H:Tyr-50-Asp is an engineered 26-10 H chain mutant that produces antibody with reduced affinity for digoxin, relative to wild-type 26-10 (Schildbach et al., 1993a).

Ascites production and antibody purification

Antibody was produced in ascites as described (Mudgett-Hunter et al., 1982). Antibodies R3 and L1B1 were purified for amino acid sequencing on DEAE-cellulose as described (Smith & Margolies, 1984).

Variable region nucleotide sequencing

Nucleotide sequencing of the V region cDNA of antibodies R3 and L1B1 by chemical cleavage was done as described (Panka & Margolies, 1987) except oligonucleotide primers complementary to L and H chain V region framework sequences were used in addition to those complementary to the V–C junction for synthesis of ^{32}P-end-labeled cDNA. The oligonucleotides hybridized to position 67–73 of the L chain ([5′d(CAGTGTGAAATC TGTCCC)3′]), and positions 40–45 ([5′d(AAGGCTCTTTC CATGGC)3′]), 66–71 ([5′d(CTACAGTCAATGTGGCC)3′]), and 82a–89 ([5′d(AGACTGCAGAATCCTCCGATGTCAGG CTGCG)3′]) of the H chain. Nucleotide sequencing of PCR-amplified V region cDNA was done as described (Schildbach et al., 1991).

Variable region amino acid sequencing

Antibody H and L chains were separated and purified as reported previously (Novotny & Margolies, 1983; Smith & Margolies, 1984). Variant R3 H chain CNBr peptides were prepared and purified by gel filtration and HPLC as described (Smith & Margolies, 1984, 1987). Variant L1B1 H chain CNBr peptides were prepared and purified by HPLC using Vydac C-4 columns (Separations Group, Hesperia, California) eluting with a linear gradient from 100% solvent A (0.1% trifluoroacetic acid [TFA] in water) to 60% solvent B (0.1% TFA in acetonitrile) over 40 or 60 min. Fully reduced and alkylated L chains were citraconylated, digested with trypsin, and purified by HPLC using either described methods (Smith & Margolies, 1984) or Vydac C-4 columns as above. Amino acid sequence analyses of purified peptides were performed on an Applied Biosystems 470A gas phase sequencer (Foster City, California) with phenylthiohydantoin analyses using on-line HPLC. Amino-terminal amino acid sequence analyses of intact H and L chains were done using a Beckman 890C sequencer with OPA treatment at selected cycles where proline was N-terminal (Brauer et al., 1984).

Antibody mutagenesis

Mutagenesis was performed according to Kunkel (1985) on the cloned rearranged 26-10 H chain V region gene as described (Schildbach et al., 1993b). The mutated V regions were cloned into an expression vector, the vectors transferred by electroporation into 26-10κ cells, and antibody-producing clones selected by screening of supernatants for digoxin binding or presence of antibody (Schildbach et al., 1993b).

Digoxin binding assays

Cell culture supernatants of 26-10, variants R3 and L1B1, and engineered 26-10 mutants were tested for the presence of antibody and for antigen binding. Serial 2-fold dilutions of cell culture supernatants in 10% γ-globulin-free horse serum (Gibco, Grand Island, New York) in phosphate-buffered saline (10% HS-PBSA) were added to wells of polyvinylchloride plates coated with goat anti-mouse-Fab antibody (ICN Immunobiologicals, Lisle, Illinois). A solution of 10% HS-PBSA was used as a negative control. The plates were incubated for 60 min at 20 °C and washed repeatedly with distilled water. A solution of goat anti-mouse-Fab antibody that had been radioiodinated by the chloramine T method (Greenwood et al., 1963) was added to the wells, and the plates were incubated for 60 min at 20 °C. The wells were washed with water, cut from the plates, and counted using a gamma counter. The dilution of each cell supernatant giving 70–80% maximal binding to the goat anti-mouse-Fab antibody-coated plates was added to wells of plates

coated with digoxin–HSA, and the plates were incubated and bound antibody was detected with radioiodinated goat anti-mouse-Fab antibody as above.

Affinity and specificity determinations

[^{3}H]digoxin used for affinity and specificity measurements was purchased from New England Nuclear (Boston, Massachusetts). Affinities were measured with a saturation equilibrium assay using filtration through glass fiber filters to separate bound and free ligand (Schildbach et al., 1991) as modified (Schildbach et al., 1993b). Specificities were determined by a solution-phase competition assay also using glass fiber filtration (Schildbach et al., 1993a). Cell supernatants were used in assays for all antibodies except mutant H:Asn-35-Asp, for which diluted ascites was used. As H:Asn-35-Asp has a relatively low affinity, higher concentrations of antibody are required for measurements.

Molecular modeling and docking

The modeling procedure (Schildbach et al., 1993b) is an adaptation of the minimum perturbation approach (Shih et al., 1985) that combines a side-chain conformational search with energy minimization to locate the lowest energy conformation of a mutated side chain. The modeling procedure has been used to successfully predict the structure of an H:Asn-35-His mutation in 26-10 (Schildbach, 1992) that is contained in 26-10R9, a mutant of 26-10 for which the crystal structure has been determined at 2.5 Å resolution to an *R*-value of 0.176 (R.K. Strong, P.D. Jeffrey, L.C. Sieker, C. Chang, R.L. Campbell, G.A. Petsko, E. Haber, M.N. Margolies, & S. Shaw, in prep.).

In modeling the mutants, we assumed that significant structural changes would be restricted to the area near the H35 residue. The results of comparison of mutants of T4 lysozyme (Eriksson et al., 1992) and chymotrypsin inhibitor 2 (Jackson et al., 1993) to their respective wild-type structures are consistent with this assumption. In the hapten docking procedure used here, we assume that the antibody does not undergo any significant rearrangement upon binding. Although such rearrangements have been noted in other antibodies (Rini et al., 1992), comparison of the X-ray crystal structures of 26-10 Fab and the 26-10 Fab–digoxin complex reveals no significant differences in antibody structure upon binding (Jeffrey et al., 1993). The only observed difference between the crystal structure of digoxin (Go et al., 1980) and the structure of digoxin complexed with 26-10 (Jeffrey et al., 1993) is a rotation of the lactone ring of approximately 180° about the C17–C20 bond. Both of these lactone orientations have been observed in other cardiac glycoside crystal structures (Go et al., 1980), but the high degree of complementarity between antibody and lactone allows only a single lactone conformation when complexed (Jeffrey et al., 1993). We assume digoxin will complex with the mutants in the same orientation as it does with 26-10. For docking experiments using dihydrodigoxigenin and oleandrin, we assumed that the steroid moiety maintains a similar orientation when complexed with antibody, but groups that differ from digoxin that are capable of free rotation (the saturated lactone of dihydrodigoxigenin and the 16-acetyl and oleandrose groups of oleandrin) were positioned by conformational search (see below). The structure of the steroid moiety of cardiac glycosides (Go & Bhandary, 1989), even when bound by antibody (Jeffrey et al., 1993), varies little, supporting this approach. The above assumptions may not be valid in all cases, causing inaccuracies in the modeling.

Parameters used for amino acids, including partial atomic charges, were as described (Novotny et al., 1989). The partial atomic charges of the hydroxyl oxygens and hydrogens and the hydroxyl-bearing carbon atoms (−0.65e, 0.4e, and 0.25e, respectively) of digoxin are taken from those for serine (Novotny et al., 1989). For the O-linked acetyl group of oleandrin, the partial atomic charges were C16 = 0.4e, O16 = −0.44e, C24 = 0.35e, O24 = −0.365e, and C25 = 0.055e (see Fig. 1 for numbering). Partial atomic charges for C17 (0.112e), C20 (0.052e), C21 (0.392e), O21 (−0.543e), C22 (−0.284e), C23 (0.873e), and O23 (−0.602e) were calculated from ab initio computations as described (Schildbach et al., 1993a). The values for bond lengths, bond angles, torsion angles, and improper torsion angles of the lactone and hydroxyl atoms were averaged from the X-ray crystal structures of digoxin and several digoxin analogues as described (Schildbach et al., 1993a).

Modeling was based on the crystal structure of the 26-10 Fab:digoxin complex (Jeffrey et al., 1993), which has been determined to a 2.5-Å resolution with an *R*-value of 0.171 and an RMS deviation from ideal bond lengths of 0.013 Å. The program CONGEN (Bruccoleri & Karplus, 1987) was used. Prior to modeling, a 26-10 Fv fragment was constructed from the 26-10 Fab:digoxin coordinates (Schildbach et al., 1993b). Digoxin was removed from the structure during the modeling procedure. A mutant side chain was introduced into the structure using the SPLICE command of CONGEN. For the Ala mutant, the model was minimized (see below) after introduction of the amino acid. For all other side chains, a conformational search using a 30° grid was performed. Maximum allowable van der Waals energy limits were +200 kcal/atom, and conformations in which this limit was exceeded were discarded. Each of the allowed conformations was subjected to a 4-step energy minimization procedure. The hydrogens of the substituted side chains were deleted, replaced with the HBUILD command of CONGEN, and energy-minimized (200 steps adopted basis Newton Rapheson minimization [ABNR]; Brooks et al., 1983) while all other atoms were fixed. This established hydrogen bonds for the substituted side chain. The modeled side chain was then fixed while the surrounding atoms were minimized (10 steps ABNR), and the modeled side-chain atoms and hydrogen atoms were then minimized while all other atoms were fixed (50 steps ABNR). The final step was a minimization (500 steps ABNR) with no restraints or constraints on the modeled side chain or on side-chain atoms with 7.5 Å of the modeled side-chain β-carbon (C_β) and moderate (4 kcal/Å) harmonic restraints on main-chain atoms with 7.5 Å of the modeled side-chain C_β. Increasing restraints were placed on all atoms except hydrogens as their distance from the modeled side-chain C_β increased (4 kcal/Å for 7.5–10 Å, 8 kcal/Å for 10–12.5 Å, and 16 kcal/Å for 12.5–15 Å). Atoms 15 Å or more from the modeled side-chain C_β were fixed. During minimization, the 1–4 nonbonded interactions were excluded from the calculated energies. Hydrogen bonds were calculated for a distance of 5 Å and a donor-H···acceptor angle of 70°, with cutoffs smoothed using a switching function (Brooks et al., 1983) in the ranges of 4.5–5 Å and 50–70°. Nonbonded interactions were calculated over an 8-Å range, with a switching function used from 7.5 to 8 Å. The dielectric constant was set to 4× the distance between atom pairs. No wa-

ter molecules were included. The lowest energy conformations were then selected for docking experiments.

Digoxin, dihydrodigoxigenin, or oleandrin was inserted into the models in the same orientation as digoxin in the X-ray crystal structure. The structure of digoxigenin was taken from the 26-10 Fab:digoxin complex crystal structure (Jeffrey et al., 1993) and oleandrin (Kartha & Go, 1981) and dihydrodigoxigenin (S-isomer; Mostad, 1982) from their crystal structures. All hapten structures were energy-minimized. Prior to minimization, the lactone of oleandrin was rotated, relative to the steroid moiety, to the position of the lactone of digoxin in the 26-10 Fab:digoxin crystal structure. The new position of the oleandrin lactone represents an allowed conformation for cardiac glycosides, but not the orientation seen in the oleandrin crystal structure. During minimization of digoxigenin and oleandrin, the lactone ring position relative to the steroid moiety was maintained using harmonic constraints. After insertion of the hapten into an antibody binding site, the lowest energy positions for hydroxyl hydrogens at the 12 position (for digoxin and dihydrodigoxigenin) and 14 position (for all haptens), and for the 16-acetyl and 3-oleandrose moieties of oleandrin, were determined by a conformational search using a 30° grid over all dihedral angles. The position of the lactone ring of dihydrodigoxigenin was determined by conformational search using a 15° grid over the C13-C17-C20-C21 dihedral angle. The antibody:hapten complex model was then energy-minimized in a 2-step process. First, the H35 side chain was minimized while all other atoms were fixed (500 steps ABNR). Then, all main-chain atoms within 12.5 Å of the hapten C8 were restrained (8 kcal/Å), all other atoms within 12.5 Å of the hapten C8 were unrestrained, and all atoms greater than 12.5 Å from C8 were fixed, and the structure was minimized (500 steps ABNR). The hapten C8 was arbitrarily chosen as center of the minimization because it is near the center of the cardenolide structure.

The diagrams of the 26-10:digoxin structure and the models were made using the plotting program PLT2 (R.E. Bruccoleri & D. States, unpubl.). Both PLT2 and CONGEN are available by request to R.E.B.

Acknowledgments

We thank Rou-fun Kwong and Lii Suen for technical assistance. We also thank Dr. Behnaz Parhami-Seren for providing the radiolabeled goat anti-mouse-Fab antibody and Dr. Emmanuel Burgeon for providing the digoxin-conjugated human serum albumin. This work was supported by National Institutes of Health grants PO1-HL19259 and RO1-HL47415. J.F.S. was supported by a National Science Foundation Graduate Fellowship, 1986-1989.

References

Alzari PM, Spinelli S, Mariuzza RA, Boulot G, Poljak RJ, Jarvis JM, Milstein C. 1990. Three-dimensional structure determination of an anti-2-phenyloxazolone antibody: The role of somatic mutation and heavy/light chain pairing in the maturation of an immune response. *EMBO J 9*:3807-3814.

Amit AG, Mariuzza RA, Phillips SEV, Poljak RJ. 1986. Three-dimensional structure of an antigen-antibody complex at 2.8 Å resolution. *Science 233*:747-753.

Arevalo J, Stura EA, Taussig MJ, Wilson IA. 1993. Three-dimensional structure of an anti-steroid Fab' and progesterone-Fab' complex. *J Mol Biol 231*:103-118.

Bentley GA, Boulot G, Riottot M, Poljak RJ. 1990. Three-dimensional structure of an idiotope-anti-idiotope complex. *Nature 348*:254-257.

Brauer AW, Oman CL, Margolies MN. 1984. Use of *o*-phthalaldehyde to reduce background during automated Edman degradation. *Anal Biochem 137*:134-142.

Brooks BR, Bruccoleri RE, Olafson BD, States DJ, Swaminathan S, Karplus M. 1983. CHARMM: A program for macromolecular energy minimization, and dynamics calculations. *J Comput Chem 4*:187-217.

Bruccoleri RE, Karplus M. 1987. Prediction of the folding of short polypeptide segments by uniform conformational sampling. *Biopolymers 26*:1337-217.

Brunger AT, Leahy DJ, Hynes TR, Fox RO. 1991. 2.9 Å resolution structure of an anti-dinitrophenyl-spin-label monoclonal antibody Fab fragment with bound hapten. *J Mol Biol 221*:239-256.

Chothia C. 1974. Hydrophobic bonding and accessible surface area in proteins. *Nature 248*:338-339.

Chothia C, Lesk A, Tramontano A, Levitt M, Smith-Gill SJ, Air G, Sheriff S, Padlan EA, Davies DR, Tulip WR, Colman PM, Spinelli S, Alzari PM, Poljak RJ. 1989. Conformations of immunoglobulin hypervariable regions. *Nature 342*:877-883.

Cygler M, Rose DR, Bundle DR. 1991. Recognition of a cell-surface oligosaccharide of pathogenic *Salmonella* by an antibody Fab fragment. *Science 253*:442-445.

Diamond B, Scharff MD. 1984. Somatic mutation of the T15 heavy chain gives rise to an antibody with autoantibody specificity. *Proc Natl Acad Sci USA 81*:5841-5844.

Eisenberg D, Wesson M, Yamashita M. 1989. Interpretation of protein folding and binding with atomic solvation parameters. *Chem Scr 29A*: 217-221.

Eriksson AE, Baase WA, Zhang X, Heinz DW, Blaber M, Baldwin EP, Matthews BW. 1992. Response of a protein structure to cavity-creating mutations and its relation to the hydrophobic effect. *Science 255*:178-183.

Fischmann TO, Bentley GA, Bhat TN, Boulot G, Mariuzza RA, Phillips SEV, Tello D, Poljak RJ. 1990. Crystallographic refinement of the three-dimensional structure of the Fab D1.3-lysozyme complex at 2.5 Å resolution. *J Biol Chem 266*:12915-12920.

Glockshuber R, Stadlmuller J, Pluckthun A. 1991. Mapping and modification of an antibody hapten binding site: A site-directed mutagenesis study of McPC603. *Biochemistry 30*:3049-3054.

Go K, Bhandary KK. 1989. Structural studies on the biosides of *Digitalis lanata*: Bisdigitoxosides of digitoxigenin, gitoxigenin and digoxigenin. *Acta Crystallogr B 45*:306-312.

Go K, Kartha G, Chen JP. 1980. Structure of digoxin. *Acta Crystallogr B 36*:1811-1819.

Greenwood FC, Hunger WM, Glover JS. 1963. The preparation of ^{131}I-labelled human growth hormone of high specific radioactivity. *Biochem J 89*:114-123.

Herron JN, He X, Mason ML, Voss EW Jr, Edmundson AB. 1989. Three-dimensional structure of a fluorescein-Fab complex crystallized in 2-methyl-2,4-pentanediol. *Proteins Struct Funct Genet 5*:271-280.

Hudson NW, Mudgett-Hunter M, Panka DJ, Margolies MN. 1987. Immunoglobulin chain recombination among anti-digoxin antibodies by hybridoma-hybridoma fusion. *J Immunol 139*:2715-2723.

Jackson SE, Moracci M, elMasry N, Johnson CM, Fersht AR. 1993. Effect of cavity-creating mutations in the hydrophobic core of chymotrypsin inhibitor 2. *Biochemistry 32*:11259-11269.

Jeffrey PD, Strong RK, Sieker LC, Chang CY, Campbell RL, Petsko GA, Haber E, Margolies MN, Sheriff S. 1993. 26-10 Fab-digoxin complex: Affinity and specificity due to surface complementarity. *Proc Natl Acad Sci USA 90*:10310-10314.

Kabat EA, Wu TT, Perry HM, Gottesman KS, Foeller C. 1991. *Sequences of proteins of immunological interest*. Washington, D.C.: U.S. Department of Health and Human Services, U.S. Government Printing Office.

Kartha G, Go K. 1981. Oleandrin. *Cryst Struct Commun 10*:1323-1327.

Kunkel TA. 1985. Rapid and efficient site-specific mutagenesis without phenotypic selection. *Proc Natl Acad Sci USA 82*:488-492.

Kussie PH, Parhami-Seren B, Wysocki LJ, Margolies MN. 1994. A single engineered amino acid substitution changes antibody fine specificity. *J Immunol 152*:146-152.

Lee BK, Richards FM. 1971. The interpretation of protein structures: Estimation of static accessibility. *J Mol Biol 119*:537-555.

Mostad A. 1982. Crystal and molecular structure of dihydrodigoxigenin hydrate. *Acta Chem Scand B 36*:635-639.

Mudgett-Hunter M, Anderson W, Haber E, Margolies MN. 1985. Binding and structural diversity among high-affinity monoclonal anti-digoxin antibodies. *Mol Immunol 22*:477-488.

Mudgett-Hunter M, Margolies MN, Ju A, Haber E. 1982. High-affinity monoclonal antibodies to the cardiac glycoside, digoxin. *J Immunol 129*:1165-1172.

Near RI, Ng SC, Mudgett-Hunter M, Hudson NW, Margolies MN, Seid-

man JG, Haber E, Jacobson MA. 1990. Heavy and light chain contributions to antigen binding in an anti-digoxin chain recombinant antibody produced by transfection of cloned anti-digoxin antibody genes. *Mol Immunol 27*:901–909.

Novotny J, Bruccoleri RE, Saul SA. 1989. On the attribution of binding energy in antigen-antibody complexes McPC603, D1.3, and HyHEL-5. *Biochemistry 28*:4735–4749.

Novotny JN, Margolies MN. 1983. Amino acid sequence of the light chain variable region from a mouse anti-digoxin hybridoma antibody. *Biochemistry 22*:1153–1158.

Padlan EA. 1990. On the nature of antibody combining sites: Unusual structural features that may confer on these sites an enhanced capacity for binding ligands. *Proteins Struct Funct Genet 7*:112–124.

Padlan EA, Silverton EW, Sheriff S, Cohen GH, Smith-Gill SJ, Davies DR. 1989. Structure of an antibody-antigen complex: Crystal structure of the HyHEL-10 Fab-lysozyme complex. *Proc Natl Acad Sci USA 86*: 5938–5942.

Panka DJ, Margolies MN. 1987. Complete variable region sequences of five homologous high affinity anti-digoxin antibodies. *J Immunol 139*:2385–2391.

Panka DJ, Mudgett-Hunter M, Parks DR, Peterson LL, Herzenberg LA, Haber E, Margolies M. 1988. Variable region framework differences result in decreased or increased affinity of variant anti-digoxin antibodies. *Proc Natl Acad Sci USA 85*:3080–3084.

Parhami-Seren B, Kussie PH, Strong RK, Margolies MN. 1993. Conservation of binding site geometry among *p*-azophenylarsonate-specific antibodies. *J Immunol 150*:1829–1837.

Rini JM, Schulze-Gahmen U, Wilson IA. 1992. Structural evidence for induced fit as a mechanism for antibody-antigen recognition. *Science 255*:959–965.

Rose DR, Przybylska M, To RJ, Kayden CS, Oomen RP, Vorberg E, Young NM, Bundle DR. 1993. Crystal structure to 2.45 Å resolution of a monoclonal Fab specific for the *Brucella* A cell wall polysaccharide antigen. *Protein Sci 2*:1106–1113.

Rudikoff S, Giusti AM, Cook WD, Scharff MD. 1982. Single amino acid substitution altering antigen-binding specificity. *Proc Natl Acad Sci USA 79*:1979–1983.

Sambrook J, Fritsch EF, Maniatis T. 1989. *Molecular cloning*. Cold Spring Harbor, New York: Cold Spring Harbor Laboratory Press.

Schildbach JF. 1992. An analysis of structural complementarity and specificity of an anti-digoxin antibody using mutagenesis and molecular modeling [thesis]. Cambridge, Massachusetts: Harvard University.

Schildbach JF, Near RI, Bruccoleri RE, Haber E, Jeffrey PD, Ng S, Novotny J, Sheriff S, Margolies MN. 1993a. Heavy chain position 50 is a determinant of affinity and specificity for the anti-digoxin antibody 26-10. *J Biol Chem 268*:21739–21747.

Schildbach JF, Near RI, Bruccoleri RE, Haber E, Jeffrey PD, Novotny J, Sheriff S, Margolies MN. 1993b. Modulation of antibody affinity by a non-contact residue. *Protein Sci 2*:206–214.

Schildbach JF, Panka DJ, Parks DR, Jager GC, Novotny J, Herzenberg LA, Mudgett-Hunter M, Bruccoleri RE, Haber E, Margolies MN. 1991. Altered hapten recognition by two anti-digoxin hybridoma variants due to variable region point mutations. *J Biol Chem 266*:4640–4647.

Sharp KA, Nicholls A, Fine RF, Honig B. 1991. Reconciling the magnitude of the microscopic and macroscopic hydrophobic effect. *Science 252*:106–109.

Sheriff S, Hendrickson WA, Smith JL. 1987a. Structure of myohemerythrin in the azidomet state at 1.7/1.3 Å resolution. *J Mol Biol 197*:273–296.

Sheriff S, Silverton EW, Padlan EA, Cohen GH, Smith-Gill SJ, Finzel BC, Davies DR. 1987b. Three-dimensional structure of an antibody-antigen complex. *Proc Natl Acad Sci USA 84*:8075–8097.

Shih HHL, Brady J, Karplus M. 1985. Structure of proteins with single-site mutations: A minimum perturbation approach. *Proc Natl Acad Sci USA 82*:1697–1700.

Smith JA, Margolies MN. 1984. Complete amino acid sequence of the heavy-chain variable region from an A/J mouse antigen-nonbinding monoclonal antibody bearing the predominant arsonate idiotype. *Biochemistry 23*:4726–4732.

Smith JA, Margolies MN. 1987. Complete amino acid sequences of the heavy and light chain variable regions from two A/J mouse antigen nonbinding monoclonal antibodies bearing the predominant *p*-azophenylarsonate idiotype. *Biochemistry 26*:604–612.

Sompuram SR, Sharon J. 1993. Verification of a model of a Fab complex with phenylarsonate by oligonucleotide-directed mutagenesis. *J Immunol 150*:1822–1828.

Stanfield RL, Fieser TM, Lerner RA, Wilson IA. 1990. Crystal structures of an antibody to a peptide and its complex with peptide antigen at 2.8 Å. *Science 248*:712–719.

Strong RK, Campbell R, Rose DR, Petsko GA, Sharon J, Margolies MN. 1991. Three-dimensional structure of murine anti-*p*-azophenylarsonate Fab 36-71. I. X-ray crystallography, site-directed mutagenesis, and modeling of the complex with hapten. *Biochemistry 30*:3739–3747.

Tulip WR, Varghese JN, Laver WG, Webster RG, Colman P. 1992. Refined crystal structure of the influenza virus N9 neuraminidase-NC41 Fab complex. *J Mol Biol 227*:122–148.

Vix O, Rees B, Thierry JC, Altschuh D. 1993. Crystallographic analysis of the interaction between cyclosporin A and the Fab fragment of a monoclonal antibody. *Proteins Struct Funct Genet 15*:339–348.

Generation of an antibody with enhanced affinity and specificity for its antigen by protein engineering

S. Roberts, J. C. Cheetham & A. R. Rees

Laboratory of Molecular Biophysics, Department of Zoology, Oxford University, The Rex Richards Building, Oxford 0X1 3QU

A detailed description of the interactions between an antibody and its epitope is necessary to allow an understanding of the way in which antibodies bind to antigenic surfaces presented by foreign molecules. Ideally this should be done by analysis of crystal structures of antibody–antigen complexes, but so far only two of these are available[1,2]. An alternative strategy[3] combines molecular modelling[4–6] with site-directed mutagenesis (SDM) and using this we have generated a preliminary model[7] of the complex between Gloop2, an antibody raised against a peptide containing the 'loop' determinant of hen egg-white lysozyme (HEL) which also binds the native protein[8], and its epitope on the protein surface. The main predictions from our model were; (1) that the surface of interaction between the antibody and the antigen is large (20 Å × 15 Å) and involves all the complementarity-determining regions (CDRs), (2) that electrostatic interactions were important in the formation of the complex, and (3) that conformational changes in either the loop or in the CDRs may occur during the formation of the complex. Here we report SDM studies which test some of these predictions; removal of two charged residues at the periphery of the combining site increases the affinity of the antibody for its antigen over 8-fold and decreases its ability to cross-react with closely-related antigens. This result is at variance with our original prediction but can be accommodated within our newly refined model; the role of electrostatics in antigen–antibody interactions is now questionable.

The antibody-combining site is formed by the juxtaposition of six hypervariable or CDRs, three deriving from the light chain (designated L1, L2 and L3) and three from the heavy chain (H1, H2 and H3). Although the structural details of a number of antibody-combining sites are known[9–14], the manner in which CDR-backbone length and sequence influences the final topology is unknown. Such information may eventually be derived from comparisons within a larger data base of structures than presently exists.

Our initial analysis of the computer model of the Gloop2-HEL complex, together with the results of binding studies of Gloop2 and a panel of variant avian lysozymes[8], strongly implicated the interaction of (1) Glu 28 (27A using the Kabat numbering system[15]), in the light chain CDR1 (L1), with Arg 68 (HEL) and (2) Lys 56, in the heavy chain CDR2 (H2), with Asn 77 (HEL). In neither case are the residue pairs close enough to form hydrogen bonds (closest contact 4.7 Å), but it was suggested that they may be important in the orientation of the two interacting protein surfaces. Based on these initial observations both Glu 28 (L1) and Lys 56 (H2) were chosen as candidates for mutagenesis. There were also a number of residues that appeared to be partially buried within the combining site, inaccessible to antigen contact and yet variable between the individual antibodies. Glu 50 in the heavy chain H2 of Gloop2 fell into this category. Four types of substitution were therefore made by SDM: Glu 28 to Ser, Lys 56 to Gln and Glu 50 to Ser and the double mutant Glu 28 to Ser: Lys 56 to Gln according to the scheme shown in Fig. 1, and the mutant proteins were expressed[16].

In parallel with the mutagenesis studies, further refinement of the initial model for the Gloop2–HEL complex was carried out by energy minimization, using the GROMOS molecular dynamics package[17]. Regions of unacceptable stereochemistry in the centre of the combining site region (Fig. 2*a*) were completely eliminated from the model by this procedure, in addition to a general enhancement of the complementarity of the antibody and antigen surfaces (Figure 2*b*). The principal contact residues, however, remain unchanged between the old and new models. The energy minimization of the complex showed that only minor conformational changes (<0.5 Å) would be required within the antibody and the antigen for the two molecules to dock together to form a complex. This is consistent with observations from the experimental study of Poljak and co-workers[1].

The results of binding assays performed with the mutant antibodies, using HEL and Pep1 (a loop-containing peptide) as antigens, are shown in Fig. 3*a* and summarized in Table 1. The single mutant Glu 28 to Ser showed a moderate increase in

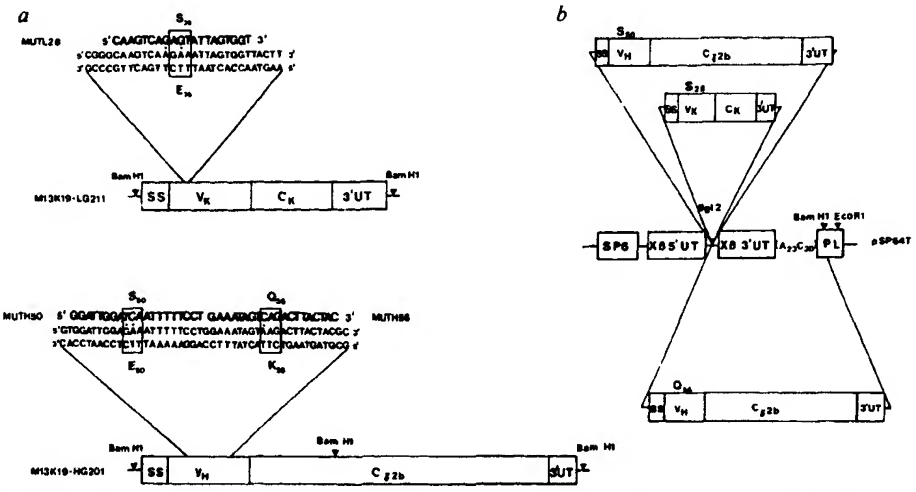

Fig. 1 *a*, The cloning of Gloop2 heavy and light chain complementary DNAs and their expression by *in vitro* transcription with SP6, and *in vivo* translation with *Xenopus* oocytes to generate fully assembled and functional antibodies has been described elsewhere[16]. The same procedure was used to express the mutant antibodies and SDM was performed using the *Eco*K/*Eco*B reciprocating selection system[19]. The cDNA clones were subcloned in an inverted orientation into the M13 mutagenesis vector (M13K19) such that the mutagenic primers were 5′ to the selection primers. Mutagenesis using the mutagenic primer, MUTL28, converted Glu 28(GAA) in CDR1 of the light chain to Ser (AGT) by three mismatches (*), the fourth being silent. The mutagenic primers MUTH50 and MUTH56 generated changes within the CDR2 of the heavy chain at position 50, converting a Glu (GAA) to a Ser (TCA) by two mismatches, and at position 56, a Lys (AAG) to a Gln (CAG) by one mismatch. *b*, Mutant RNA transcripts were synthesized by subcloning the mutated cDNA clones as *Bam*H1 fragments into the *Bgl*II or *Bgl*II/*Bam*H1-restricted vector, pSP64T. All constructs were linearized by *Eco*R1 restriction. The single mutant antibodies, E28S, E50S and K56Q were prepared by comicroinjection of the mutant RNA transcript with the appropriate 'wild-type' heavy or light chain RNA transcript into the cytoplasm of *Xenopus* oocytes; the double mutant E28SK56Q was produced by microinjection of the two mutant transcripts of E28S and K56Q. SS, signal peptide sequence; V, variable region and C, constant region of either the light (κ) or γ2b heavy chain (H); UT, untranslated region; SP6, promoter region from *Salmonella typhimurium* phage; X-UT, the 5′ and 3′ UT regions of the *Xenopus* β-globin gene; PL, polylinker.

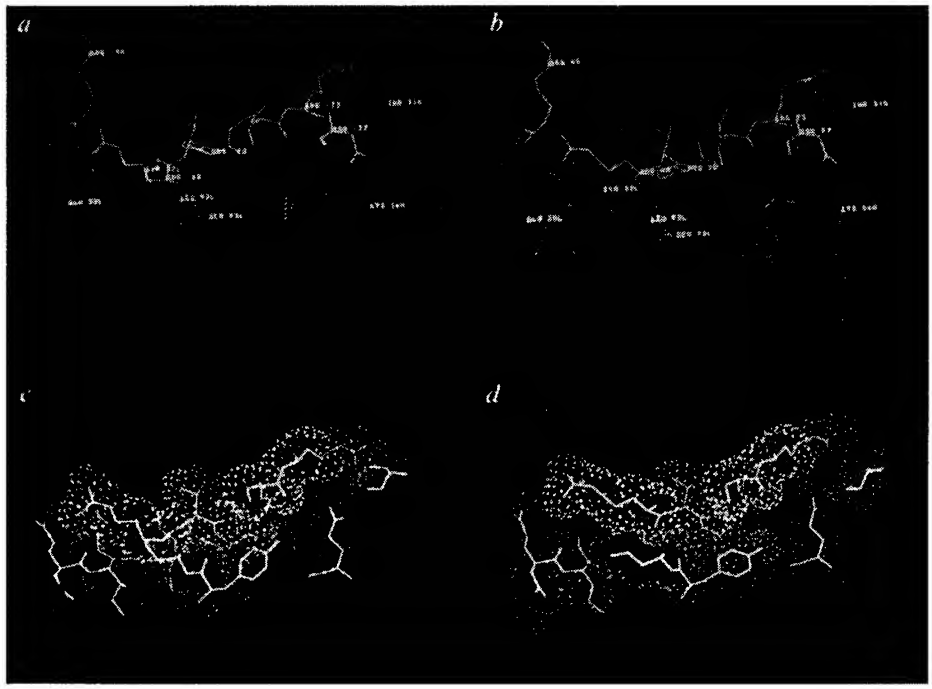

Fig. 2 Combining site region of the Gloop2/HEL complex[7] before (*a*) and after (*b*) refinement of the model by energy minimization. In *a*, note the unacceptably close contacts between (1) main-chain atoms in the region of Leu 92 and Ser 93 of L3, and (2) side-chain atoms in the region of Tyr 32(L1) and Pro 70(HEL). In panel *b*, these bad contact regions are no longer present and the complementarity of the two molecular surfaces is clearly improved. The improvement in the model resulting from the energy minimization was reflected in the large potential energy (p.e.) drop over the 164 cycles of steepest descent minimization: p.e. (initial model) = $+2.95\times10^{11}$ kcal mol^{-1}; p.e. (minimized model) = -0.533×10^{4} kcal mol^{-1}. A van der Waals representation of the antibody (blue): antigen (green) surfaces (*c* shows model *a*, and *d* shows model *b*) indicates the general stereochemical complementarity of the two molecules in the region of the combining site. Hydrogen bonds, both within the individual molecules themselves, and between antigen and antibody, are indicated (- - -).

Table 1 Affinity constants (k_D/M) for binding of Gloop 2 and its mutants to Pep1 and HEL

	Gloop 2	E28S	K56Q	E28SK56Q
Pep1	$2.0\pm0.75\times10^{-8}$	8.2×10^{-9}	2.0×10^{-8}	4.8×10^{-9}
HEL	$2.3\pm1.0\times10^{-7}$	4.7×10^{-8}	$1.9\pm0.12\times10^{-7}$	$2.75\pm0.02\times10^{-8}$

Assays were carried out in triplicate as described in Roberts and Rees[16]. Essentially microtitre plates were coated with goat anti-mouse IgG antibody (affinity purified) at a concentration of 50 μg ml^{-1} in PBS for 18 h at 4 °C. After coating the plates were blocked with PBS containing 0.05% Tween for 30 min at 4 °C, then 2 × 1 min at room temperature. Oocyte test supernatant was added and incubated at room temperature for 6 h. Plates were washed and ^{125}I-labelled Pep1 with and without inhibitor was added and incubated at room temperature for a further 6 h. Plates were washed with PBS/Tween 3 × 1 min and individual wells cut out and counted. The k_D values for Pep1 inhibition of ^{125}I-labelled Pep1 binding were obtained from Scatchard analysis. As Scatchard analysis was inappropriate for analysis of HEL inhibition of Pep1 binding, k_D values were obtained by the following method. Using the program SANCOL (R. Ryan, unpublished) a non-linear regression procedure[22] was used to fit the binding equation which relates specifically bound units (for instance c.p.m.—the measured variable) and the total ligand concentration (the control variable) to the experimental data [23]. Scatchard estimates of the k_D and total site concentration (S_T) values were then used as a start point for an iterative procedure which calculated the final k_D and S_T values. Binding data were measured at *p*H 7.2. The range of means obtained in different experiments is given.

Table 2 Relative affinities of Gloop 2 and its mutants for lysozymes of different species

	Gloop 2	E28S	K56Q	E28SK56Q
TEL	0.5	3.0	0.5	7
BWQEL	124	111	ND	235
RNPEL	13	ND	12	30
HuL	370	ND	ND	1300

The numbers shown express ID_{50} values for inhibition of binding of ^{125}I-labelled Pep 1 to antibody by the appropriate variant lysozyme (methods as described in the legend to Table 1). Each value has been normalized to the ID_{50} value for binding of the appropriate antibody to HEL. Variant lysozymes used in this study are: TEL, turkey egg lysozyme; BWQEL, bobwhite quail egg lysozyme; RNPEL, ring-necked pheasant egg lysozyme, and HuL, human lysozyme.

affinity for both Pep1 and HEL (3-4 fold) whereas the mutant Lys 56 to Gln showed no significant change in binding. But combining the two single mutations within the same antibody gave a double mutant which showed a marked increase in affinity for HEL (8–9-fold), and a moderate increase for Pep1 (4–5-fold) (Fig. 3*a*).

When this analysis was extended to the variant lysozymes (Table 2) the pattern of binding satisfied the purely thermodynamic criteria that, if the mutations improved the complementarity of Gloop2 for its native antigen HEL, then the variant lysozyme with the highest affinity, but non-identical complementarity, for wild type Gloop2 should experience the most drastic loss of affinity (6–7-fold decrease in relative affinity for TEL, Table 2). By contrast, those variant lysozymes with somewhat lower affinities, and hence rather less stringent interactions, would be less affected (2–4-fold decrease in relative affinity for BWQEL, RNPEL and HuL, Table 2). The double mutant thus showed not only a greater affinity for HEL, but also an increased specificity towards HEL over the other avian species. Modelling of these amino-acid changes in the antibody L1 and H2 CDRs suggests that the removal of the electrostatic residues, and their replacement by non-charged hydrophilic residues, allows a closer fit of antibody and antigen. As a consequence there is a general improvement in hydrogen bonding between the two surfaces, but without significant changes in the interactions within the antibody CDR's at the sites of the mutations (Fig. 3*b*).

By contrast, mutation of the partially-buried Glu 50 in H2 resulted in abolition of binding between the antibody and HEL or Pep1 (Fig. 3*c*). The residue in this position is the first to emerge from the framework region preceding CDR H2 and shows a high variability between heavy chains of the same V_HII subgroup[15]. In the model this residue appears to be both hydrogen bonded to Tyr 94 in neighbouring CDR L3 and involved in a salt-bridge-like interaction with Arg 101 of H3. Substitution at this position would be predicted to cause a significant change in the relative conformations of adjacent, interacting CDR's. Such perturbations, if they occurred, could more than account for the observed loss of binding. This observation may be an example of a situation where the existence of variability between antibodies at a particular residue position does not necessarily signify a minor structural role for that position in the combining

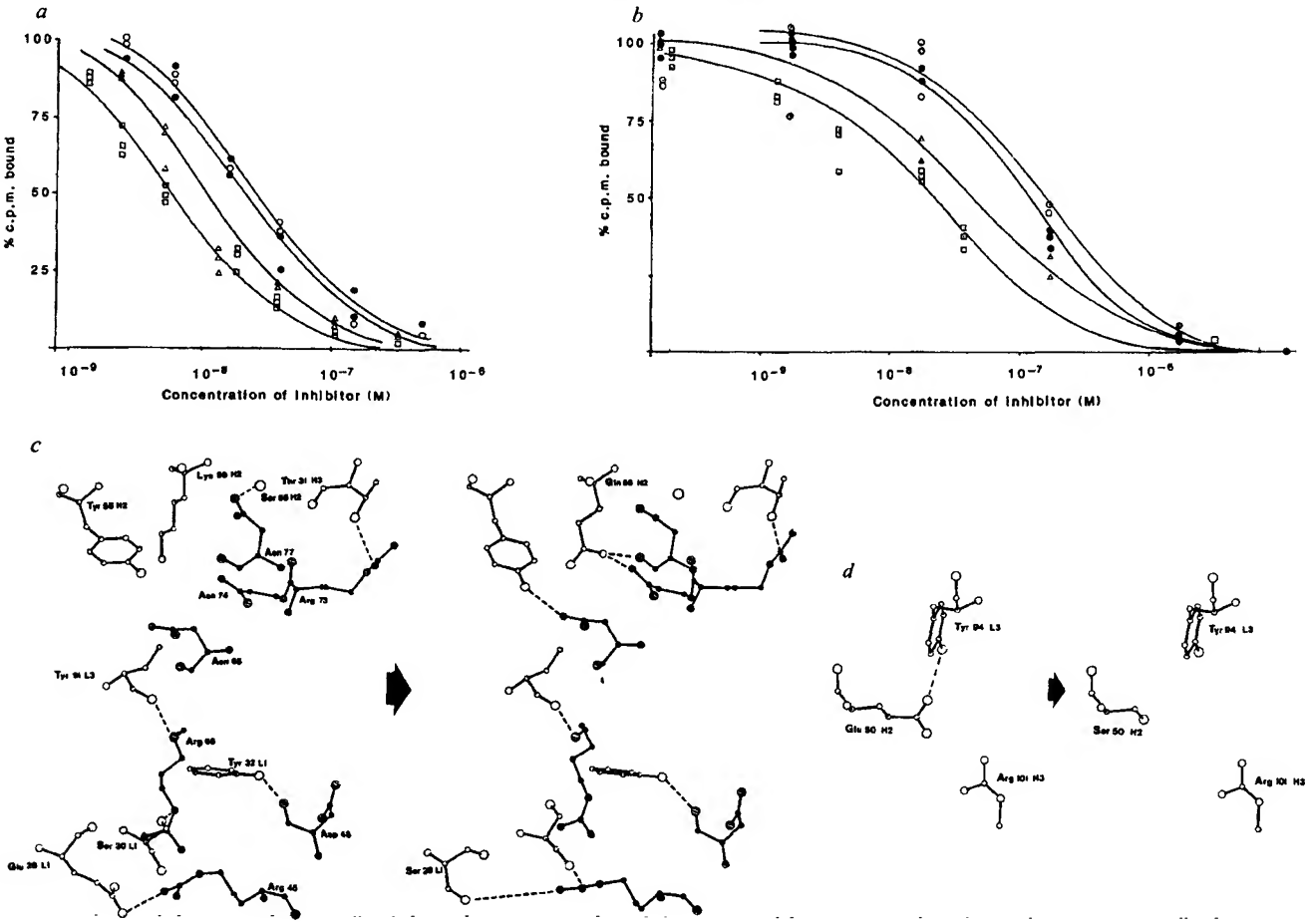

Fig. 3 Inhibition of binding of ^{125}I-labelled Pep1 to Gloop2 (○) and mutant antibodies, k56Q (●), E28S (△) and E28S K56Q (□) by *a*, Pep1 and *b*, HEL. *c*, Predicted effect of the combined mutations Glu 28-Ser (L1) and Lys 56-Gln, in the region of the antibody combining site. The modelling would suggest that hydrogen bonding interactions (- - - -) within the antibody CDR would be preserved, and in addition interactions with the antigen enhanced; Asn 65(HEL) → Tyr 58(H2), Asn 74(HEL) → Gln 56(H2), Asn 77(HEL) → Gln 56(H2), Arg 45(HEL) → Ser 28(L1) and Arg 45(HEL) → Ser 30(L1) all appear as new contacts. *d*, Predicted effect of the mutation Glu 50 → Ser (H2). Here the modelling suggests the replacement of the glutamic-acid residue by a serine will have a significant effect on the nature of the antibody-combining site, with the loss of two important interactions: (1) a hydrogen bond between Tyr 94 OH(L3) and Glu 50 OE1 (H2) and (2) a salt-bridge-like interaction between Glu 50 (H2) and Arg 101(H3). Amino-acid changes were incorporated into the model by introducing the new side chains with FRODO[20] on the PS300, and then energy minimizing the entire structure, using GROMOS[17], to obtain a model for the mutant protein[21].

site. Different combinations of CDR may have requirements for specific inter-CDR interactions. Thus, when assessing the structural consequences of somatic mutations *in vivo* or *in vitro*, both antigen-antibody and CDR-CDR interactions should be considered.

These preliminary results therefore raise two important questions concerning antibody-antigen interactions, and suggest a number of possible mutations for further study. Our original premise was that the two charged groups lying at opposite edges of the combining site (Glu 28 and Lys 56) were important contacts in the antigen interaction and, further, might actually play a role in orientating the loop region of HEL. But the engineering of an antibody with enhanced affinity for its antigen by the removal of these proposed 'key' electrostatic residues, and their replacement by non-charged polar residues, questions this hypothesis. Our results would indicate that the hydrogen-bonding between the two molecules over the combining site surface is of paramount importance. The electrostatic residue in the antigen (Arg 68), no longer paired across the interface after mutagenesis, is easily accessible to solvation by water molecules. In support, recent binding data show: (1) there is no difference in the k_{on} values for the binding of Pep1 to Gloop2 over the ionic strength range 0.01 M to 0.5 M, such as might be expected if electrostatic orientation was important in acquisition of the complex, (2) the k_D for binding of Pep1 to Gloop2 actually decreases with ionic strength from 1.15×10^{-8} M (at 0.01 M) to 3.8×10^{-9} M (at 0.50 M). As k_{on} is unchanged this result indicates that the charged residues actually exert an inhibitory effect on binding, and that when their effective charge is screened improved protein-protein contacts are possible. This proposition is consistent with the mutation experiment where the removal of the charges results in increased affinity. The possible counter-argument that, by substitution of two charged residues the surface has been rendered more 'sticky' by altering its hydrophobic/hydrophilic character is not tenable because solvent accessibility calculations[18] suggest that the hydrophilic character is largely unchanged by the substitutions Lys 56 to Gln and Glu 28 to Ser (SA < 30 Å^2).

In conclusion, we have demonstrated that it is possible to engineer an anti-peptide antibody in such a way that its affinity for the same epitope in the native protein is increased and, concomitantly, its cross-reactivity with related antigens is reduced. Inspection of the refined model suggests additional mutations that may lead to further improvements in affinity.

This approach offers a possible solution to the problem of how to generate high affinity antibodies against intact antigens when peptides are used as immunogens and thus has far-reaching therapeutic consequences.

We thank the Science and Engineering Research Council (SERC) (S.R.) and the SERC/Industry Protein Engineering Programme (J.C.) for financial support. We also thank Stuart Bradford for help with the generation and characterization of one of the mutant antibodies, Professor R.J.P. Williams for useful discussions concerning the analysis of the binding data and Professor Sir David Phillips for continued support.

Received 26 March, accepted 2 June 1987.

1. Amit, A. G., Mariuzza, R. A., Phillips, S. E. V. & Poljak, P. J. *Science* **233**, 747-753 (1986).
2. Colman, P. M. *et al. Nature* **326**, 358-363 (1987).
3. Rees, A. R. & de la Paz, P. *Trends Biochem.* **123**, 144-148 (1986).
4. Davies, D. R. & Padlan, E. A. in *Antibodies in Human Diagnosis and Therapy* 119-132 (Raven, New York, 1976)
5. Greer, J. *J. molec. Biol.* **153**, 1027-1042 (1981).
6. Novotny, J., Bruccoleri, R. & Karplus, M. *J. molec. Biol.* **177**, 787-818 (1984).
7. de la Paz, P., Sutton, B. J., Darsley, M. J. & Rees, A. R. *EMBO J.* **5**, 415-425 (1986).
8. Darsley, M. J. & Rees, A. R. *EMBO J.* **2**, 383-392 (1985)
9. Segal, D., Padlan, E., Cohen, G., Rudikoff, S., Potter, M. & Davies, D. *Proc. natn. Acad. Sci. USA* **71**, 4298-4302 (1974).
10. Epp, O., Lattman, E., Schiffer, M., Huber, R. & Palm, W. *Biochemistry* **14**, 4943-4952 (1975).
11. Saul, F., Amzel, L. & Poljak, R. *J. biol. Chem.* **253**, 585-597 (1978).
12. Marquart, M., Deisenhofer, J., Huber, R. & Palm, W. *J. molec. Biol.* **141**, 369-391 (1980).
13. Furey, W., Wang, B. C., Yoo, C. S. & Sax, M. *J. molec. Biol.* **167**, 661-692 (1983).
14. se Won Suh, *et al. Proteins* **1**, 74-80 (1986)
15. Kabat, E. A., Wu, T. T., Bilofsky, H., Reid-Miller, M. & Perry, H. *Sequences of Proteins of Immunological Interest.* (U.S. Department of Health and Human Services, National Institutes of Health, Bethesda, 1983).
16. Roberts, S. R. & Rees, A. R. *Protein Engng* **1**, 59-65 (1986)
17. Aqvist, J., van Gunsteren, W. F., Leijonmarck, M. & Topia, O. *J. molec. Biol.* **183**, 461-477 (1985).
18. Richards, F. M. *Adv. Biophys. Bioeng.* **6**, 151-176 (1977)
19. Carter, P., Bedouelle, M. & Winter, G. *Nucleic Acid Res.*, **13**, 4431-4443 (1985).
20. Jones, T. A. *Computational Crystallography* 303 (Clarendon, Oxford, 1982).
21. Shih, H. H. L., Brady, J. & Karplus, M. *Proc. natn. Acad. Sci. U.S.A.* **82**, 1697-1700 (1985).
22. Duggleby, R. G. *Analyt. Biochem.* **110**, 9-18 (1981).
23. Munson, P. J. & Rodbard, D. *Analyt. Biochem.* **107**, 220-239 (1980).

Interaction of an embryo DNA binding protein with a soybean lectin gene upstream region

K. Diane Jofuku, Jack K. Okamuro & Robert B. Goldberg*

Department of Biology, University of California, Los Angeles, California 90024, USA

Seed protein genes are highly regulated during the soybean life cycle[1,2]. These genes encode prevalent mRNAs that accumulate and decay during embryogenesis, and are either undetectable or present at low levels in mature plant organ systems[2,3]. Transcriptional activation and repression processes are important in regulating seed protein gene developmental expression programs[1,2]. We started DNA binding protein studies with the soybean lectin gene[4-6] to begin to identify *trans*-acting proteins and *cis*-regulatory sequences required for seed protein gene expression. We have identified an embryo DNA binding protein that interacts with specific sequences in the lectin gene 5′ region. The DNA binding protein is undetectable in mature plant organ systems and its concentration parallels the lectin gene transcription rate during embryogenesis. The DNA binding protein activity corresponds to a 60,000 M_r (60K) nuclear protein, and a protein of similar size interacts with at least one other seed protein gene but not with a gene inactive during embryogenesis. Our data suggest that the 60K protein, and the DNA sequences that it interacts with, may be involved in regulating lectin gene expression.

Figure 1*a* schematically shows the lectin gene region. We isolated this region as a 17.1-kilobase (kb) *Eco*RI fragment from a λCharon 4 soybean genomic library[4,7]. In addition to the lectin gene, the 17.1-kb fragment contains at least four nonseed protein genes[6]. Figure 1*b* shows the lectin gene and relevant reference sequences[5]. The lectin gene is intronless, encodes a 1.1-kb mRNA, and is expressed during specific embryonic periods and in the mature plant root[6]. *In situ* hybridization studies showed that lectin mRNA is represented primarily in embryo cotyledon cells and in root ground meristem tissue (L. Perez-Grau and R.B.G., unpublished data). By contrast, the nonseed protein genes are expressed throughout embryogenesis and in mature plant leaf, root, and stem cells[6]. Thus the lectin gene is regulated temporally and spatially during the soybean life cycle, and is embedded in a domain with several differentially expressed genes.

We isolated nuclear proteins from mid-maturation stage embryos, 75 days after flowering (DAF)[8] and then reacted these proteins with lectin gene fragments to identify *cis*-elements and *trans*-factors that are involved in regulating lectin gene expression. At mid-maturation, cell division has ceased, embryo cells are expanding and accumulating seed proteins, and lectin mRNA is ~0.75% of the embryo mRNA mass[4,8]. Figure 1*c* shows the results of a DNA gel electrophoresis mobility retardation assay[9] using a lectin gene 5′ probe (Lel 5′, Fig. 1*b*). We used this probe initially because gene transfer studies showed that the lectin gene is regulated correctly in tobacco[6], and that 0.50 kb of 5′ sequence (pLe1Δ0.5, Fig. 1*a*) is sufficient to program its expression during seed development (J.K.O. and R.B.G., unpublished results). As seen in Fig. 1*c*, Lel 5′ probe mobility was retarded significantly in the presence of nuclear proteins indicating that protein-DNA complexes formed (lanes NP and O). Addition of unlabelled poly(dI-dC)·poly(dI-dC) duplex DNA to eliminate nonspecific protein-DNA interactions[9] yielded a free Lel 5′ fragment (circle, Fig. 1*c*) and a more slowly migrating protein-DNA complex (arrow, Fig. 1*c*). Figure 1*d* shows that we were unable to detect a protein-DNA complex with a lectin gene 3′ probe (Lel 3′, Fig. 1*b*). Nor was a complex detected with a gene that is not expressed in soybean embryos (leghaemoglobin 5′, Fig. 1*d*). We added unlabelled lectin DNA (pH4.4, Fig. 1*a*), as well as unlabelled pBR322 and *Drosophila* blastoderm gene DNAs, to determine if the protein-DNA complex was specific for the lectin gene. Only the unlabelled lectin DNA eliminated the protein-DNA complex formation (Fig. 1*e*). Together, these data show that embryo nuclear protein forms a specific complex with the lectin gene, and that the protein-DNA interaction occurs in a 5′ gene region.

We reacted the Lel 5′ probe (Fig. 1*b*) with nuclear proteins from embryos at different developmental stages, and from mature plant organ systems, to test whether the DNA binding protein activity correlated with lectin gene transcription levels. The mobility retardation assay in Fig. 2*a* shows that a protein-DNA complex (arrow) was obtained with the nuclear protein extract of 25-DAF embryos (lane DAF 25) demonstrating that lectin DNA binding protein activity is present early in embryogenesis. We also obtained a protein-DNA complex with similar electrophoretic mobility using the nuclear protein extract from 40-DAF embryos (Fig. 2*a*, lane DAF 40); however, the proportion of Lel 5′ probe in the complex increased significantly. By contrast, the fraction of Lel 5′ probe in the protein-DNA complex decreased with the 75-DAF embryo nuclear protein extract (Fig. 2*a*, lane DAF 75) and was reduced to an undetectable level with nuclear proteins from embryos in the terminal stages of development (Fig. 2*a*, lane DAF 100). In addition, we were unable to detect a protein-DNA complex with leaf, stem, and root nuclear proteins (Fig. 2*a*, lanes L, S, R).

We presented elsewhere the relative lectin gene transcription rates and mRNA levels during different stages of the soybean life cycle[2,6]. Lectin mRNA accumulates and decays during embryogenesis and is undetectable in mature plant leaf and stem. Root lectin mRNA is 10^4-fold less prevalent than embryo lectin mRNA at mid-embryogenesis (40-75 DAF). Runoff tran-

* To whom correspondence should be addressed.